WATER RESOURCES RESEARCH, VOL. 35, NO. 7, PAGES 1987–2006, JULY 1999

Stochastic analysis of virus transport in aquifers

Linda L. Campbell Rehmann[1] and Claire Welty

School of Environmental Science, Engineering, and Policy, Drexel University, Philadelphia, Pennsylvania

Ronald W. Harvey

Water Resources Division, U.S. Geological Survey, Boulder, Colorado

Abstract. A large-scale model of virus transport in aquifers is derived using spectral perturbation analysis. The effects of spatial variability in aquifer hydraulic conductivity and virus transport (attachment, detachment, and inactivation) parameters on large-scale virus transport are evaluated. A stochastic mean model of virus transport is developed by linking a simple system of local-scale free-virus transport and attached-virus conservation equations from the current literature with a random-field representation of aquifer and virus transport properties. The resultant mean equations for free and attached viruses are found to differ considerably from the local-scale equations on which they are based and include effects such as a free-virus effective velocity that is a function of aquifer heterogeneity as well as virus transport parameters. Stochastic mean free-virus breakthrough curves are compared with local model output in order to observe the effects of spatial variability on mean one-dimensional virus transport in three-dimensionally heterogeneous porous media. Significant findings from this theoretical analysis include the following: (1) Stochastic model breakthrough occurs earlier than local model breakthrough, and this effect is most pronounced for the least conductive aquifers studied. (2) A high degree of aquifer heterogeneity can lead to virus breakthrough actually preceding that of a conservative tracer. (3) As the mean hydraulic conductivity is increased, the mean model shows less sensitivity to the variance of the natural-logarithm hydraulic conductivity and mean virus diameter. (4) Incorporation of a heterogeneous colloid filtration term results in higher predicted concentrations than a simple first-order adsorption term for a given mean attachment rate. (5) Incorporation of aquifer heterogeneity leads to a greater range of virus diameters for which significant breakthrough occurs. (6) The mean model is more sensitive to the inactivation rate of viruses associated with solid surfaces than to the inactivation rate of viruses in solution.

1. Introduction

The transport of colloids (particles approximately 10^{-2} to 10 μm in diameter, including viruses and bacteria as well as abiotic colloids) in groundwater has been recognized as a potential environmental problem for over 20 years [e.g., *Gerba et al*., 1975; *Wollum and Cassel*, 1978; *Yates et al*., 1985]. Virus transport, often believed to be limited to the immediate vicinity of sources such as septic tanks, can become a large-scale problem under certain circumstances. Several studies completed since the 1970s have demonstrated that viruses and bacteria can travel on the order of several hundred meters in some aquifers. Large-scale colloid transport studies are summarized in Table 1, which indicates that colloids have been observed to travel as far as 1600 m.

The potential for such large-scale transport of pathogenic viruses and bacteria through shallow drinking water aquifers is a significant public health concern [*Hurst et al*., 1997, chapter 66], especially as potable water sources become more limited [e.g., *New Jersey Department of Environmental Protection*, 1996]. Pathogens from land-disposed wastes can contaminate water supply wells, leading to waterborne disease outbreaks [*Craun*, 1985]. By recent estimates, approximately 20–25% of the groundwater sources of the United States are contaminated with microbial pathogens [*Macler*, 1995], including more than 100 types of viruses. The U.S. Environmental Protection Agency (EPA) draft groundwater disinfection rule proposes that public water systems be required to disinfect source water unless natural disinfection (i.e., natural attenuation due to sorption, filtration, and inactivation) can be demonstrated [*U.S. Environmental Protection Agency*, 1992; *Macler*, 1995]. *Macler* [1995] notes that hydrogeological factors affecting virus inactivation, travel times, and distances from contamination sources to wells must be taken into consideration when determining the degree of natural disinfection in a given aquifer. In order to designate suitable well setback distances from possible contamination sources, there is a need to develop tools to quantitatively predict the extent of potential pathogenic transport. In addition, preferential flow paths or "macropores" and the size exclusion effect (in which colloids, unable to fit into smaller pores, are limited to transport in larger ones) are recognized as having a significant effect on colloid transport [*Bales et al*., 1989; *Toran and Palumbo*, 1992; *McKay et al*., 1993a]. These observations suggest that heterogeneity plays an important role in transport at the local (of the order of a meter or less) scale. Therefore, to address larger-scale virus transport

[1]Now at Hammonton, New Jersey.

Paper number 1999WR900059.
0043-1397/99/1999WR900059$09.00

Table 1. Observed Large-Scale Colloid Transport Distances

Reference	Colloid and Diameter	Maximum Travel Distance, m	Location	Aquifer Material, Thickness	Hydraulic Conductivity, m d^{-1}	Mean Pore Velocity, m d^{-1}	Colloid Velocity, m d^{-1}
Fletcher and Myers [1974]	phage T4	1600	Missouri	carbonate rock			
Noonan and McNabb [1979]	phages T4, ϕX 174	920	New Zealand	gravel			
Martin and Noonan [1977]	Bacillus sterothermophilus	900	New Zealand	gravel	O* 10^4	≥164	200 m/d
Anan'ev and Demin [1971]	Escherichia coli bacteria	350–830	Kazakhstan	sand with gravel, pebbles, 4–8 m	O* 10^5	160	
Martin and Thomas [1974]	type 2 Aerobacter aerogenose 243, 0.015 μm	680	Great Britain	sandstone		36–180	
Vaughn and Landry [1977]	Coxsackie B3 and unidentified	408	Babylon, N. Y.	coarse sand with fine gravel			
Aulenbach [1979]	phage	400	Lake George, N. Y.	fine sand with some gravel, coarse sand	4.6–19.5	3–12	
Skilton and Wheeler [1988]	Serratia marcescens, 0.05 μm; Enterobacter cloacae, 0.1 μm	122–366	Great Britain	fractured chalk			
Idelovitch et al. [1979]	Poliovirus 1, 2, 3	60–270	Dan Region, Israel	sandstone, silt, clay			
Koerner and Haws [1979]	Poliovirus, Coxsackie B3 and echovirus	250	Vineland, N. J.	Cohansey sand with coarse gravel			
Schaub and Sorber [1977]	coliphage f2, indigenous enteroviruses, fecal streptococcus	183	Fort Devens, Mass.	silty sand and gravel	8.6		
Vaughn and Landry [1977]	echovirus 6, 21, 24, and 25 and unidentified viruses	45.7	Holbrook, N. Y.	coarse sand with fine gravel, 1–2% silt			

*Order of magnitude estimated from given velocity and hydraulic gradient values.

problems in real sediments, it would seem logical that naturally heterogeneous conditions be incorporated in formulating predictive models.

Owing to practical constraints, detailed injection and recovery field experiments investigating subsurface virus transport usually have involved travel distances less than 20 m. Nonetheless, in situ studies have yielded significant insight into colloid transport under heterogeneous conditions. Recent work has focused on identifying the effects of solution chemistry [e.g., *Bales et al*., 1995, 1997], aquifer mineralogy [*Scholl and Harvey*, 1992], heterogeneities (including fractures) [*McKay et al*., 1993a, b; *Harvey et al*., 1993], and the presence of sewage-derived organic matter [*Pieper et al*., 1997] on virus and bacteria transport. The work by *Pieper et al*. [1997] shows that the presence of sewage-derived organic matter, which often accompanies pathogens in groundwater plumes, promotes the reversibility of virus attachment to the soil grains thus potentially enhancing virus transport. *Scholl and Harvey* [1992] found that although changes in groundwater pH and soil grain surface coatings significantly affect bacterial transport in uncontaminated groundwater, effects are much less pronounced for bacteria in sewage-contaminated groundwater.

Although extensive work has been carried out to model colloid transport in laboratory columns [*Jin et al*., 1997; *Johnson et al*., 1996; *Sim and Chrysokopolous*, 1996; *Saiers et al*., 1994; *Hornberger et al*., 1992; *Tim and Mostaghimi*, 1991] and at the small field scale [*Harvey and Garabedian*, 1991], incorporation of a stochastic approach to model large-scale transport in aquifers has not been previously attempted. *Yates* [1995] compared model output of the early EPA-sponsored model VIRALT [*Park et al*., 1991] to field data obtained at several sites. The model (which assumes a homogeneous saturated zone) consistently underestimated observed virus concentrations, in some cases by several orders of magnitude. In order to account for the effects of heterogeneity on bacterial transport over small scales in a Cape Cod aquifer, *Harvey and Garabedian* [1991] successfully employed a two-zone model which accounted for layers of differing hydraulic conductivities. Several investigators have employed a colloid filtration model to simulate local-scale colloid transport in groundwater [e.g., *Saiers et al*., 1994; *Martin et al*., 1992; *Harvey and Garabedian*, 1991], an approach used in this work.

Because porous medium heterogeneities have been found to significantly affect colloid transport in laboratory and small-scale field experiments, a number of researchers have suggested that a stochastic approach may be appropriate for modeling microbial transport over larger scales. For example, *Harvey* [1991] states that "... the modeling of transport over longer [e.g., greater than 10 m] distances or thicknesses of the aquifer would necessitate a stochastic approach because it would be difficult to define aquifer structure deterministically at a larger scale." *Hornberger et al*. [1992] assert that "... the current thinking is that a stochastic description of the spatiotemporal variation of the material properties must be obtained [in order to determine field-scale dispersivities]. This may be the direction that will be appropriate for describing the parameters controlling bacterial transport in porous media as well ...." *Yates and Yates* [1990] also note the potential importance of subsurface variability in microbial transport, indicating that the cost and time involved in a detailed aquifer

characterization can be prohibitive and that other methods of modeling subsurface transport might be more appropriate. On the basis of such observations we believe that a stochastic modeling approach is warranted and important for predicting virus transport at scales of tens to hundreds of meters. The premise of this paper is that a stochastic modeling approach, incorporating natural subsurface variability, can lead to an improved mathematical representation of large-scale virus transport. Furthermore, we believe that this approach can shed light on the interaction between aquifer heterogeneity and known local-scale virus transport phenomena and the resulting influence on derived large-scale "effective" virus transport parameters. Although there is debate over whether or not virus transport models can be used to determine the degree of natural disinfection, a model incorporating the natural variability in aquifer materials and the effects on virus transport would clearly be more realistic than the simplified models [e.g., *Park et al*., 1991] currently in use.

Spectral perturbation analysis [*Gelhar*, 1993] is the methodology chosen to develop the stochastic model. In this approach the current understanding of local-scale virus transport phenomena is linked with a three-dimensional, random hydraulic conductivity distribution as the driving process in deriving upscaled or mean equations for free and attached viruses and their effective or field-scale parameters. The spectral perturbation approach does have a number of inherent assumptions that limit its applicability. Local stationarity must apply, indicating that concentration gradients are assumed to be locally constant, and perturbations in the dependent variables and parameters must be small. Ergodicity must also be invoked, so that the averaging distance of a parameter must be much larger than the correlation scale of the process (in this case, the ln K field). Finally, conditions must be amenable to an infinite domain model. If boundary conditions are important, the model must be modified in order to incorporate these effects [e.g., *Li and McLaughlin*, 1991, 1995]. Both the ergodicity and stationarity assumptions required by the mathematical technique imply that the results are applicable only to large-distance, large travel time problems. In this paper, because the total mass in a virus plume is changing over travel distance owing to inactivation, detachment, and attachment, a time variable transformation must be invoked in order for the ergodicity assumption to hold [see, e.g., *Miralles-Wilhelm and Gelhar*, 1996b]. It is important to note that while the set of mathematical assumptions and approximations of the spectral approach may appear to be severe, such constraints allow the dominant effects to be ascertained in an analytical or semianalytical form. Often the restrictions that are invoked mathematically to obtain a solution have, in fact, been found to be allowed to be relaxed in numerical validating tests [see, e.g., *Tompson and Gelhar*, 1990; *Ababou et al*., 1989]. There is a large body of literature that clearly shows that stochastic methods have proven to be effective in accounting for field-scale variability [e.g., *Gelhar*, 1993; *Dagan*, 1989] in evaluation of large-scale flow and contaminant transport problems. Several well-known examples in the literature include evaluation of macrodispersion of an ideal tracer [*Gelhar and Axness*, 1983], unsaturated flow [*Mantoglou and Gelhar*, 1987a, b, c], biodegradation of a solute [*Miralles-Wilhelm and Gelhar*, 1996b], and density-coupled transport [*Welty and Gelhar*, 1991]. In these applications of the spectral perturbation approach, assumption of a simple local-scale model has resulted in predictions of field-scale behavior that differs significantly from that predicted by the local model and in many cases has better reflected observations of flow and transport at the field scale. On the basis of this previous experience we hypothesize that incorporation of spatial variability into a virus transport model will also result in predictions of virus transport that differ significantly from those of a homogeneous local-scale model applied to a larger scale.

The purpose of this work is to incorporate spatial variability in both physical aquifer parameters and in virus transport parameters (attachment, detachment, and inactivation) in a large-scale transport model and to evaluate the effect of such variability on subsurface virus transport. Questions to be answered in this paper include the following: (1) How does incorporation of subsurface heterogeneity lead to predictions in large-scale virus transport that differ from predictions made by models developed for homogeneous media? (2) Does the stochastic approach offer insight into previous observations of field-scale virus transport under heterogeneous conditions? This research focuses on the transport of viruses with diameters of the order of 0.02–0.2 μm subject to first-order inactivation. The derived model can be simplified and applied to the transport of abiotic colloids in groundwater by setting the inactivation term to zero. This model may also be used to simulate large-scale transport of nonmotile bacteria under no-growth conditions. However, it is recognized that physiological changes during large-scale transport may result in temporal changes in bacterial attachment, settling, size, and morphology. Consideration of bacterial growth and motility would increase the complexity and nonlinearity of the model and is beyond the scope of this work.

2. Methodology

2.1. Governing Local Equations

The relevant phenomena affecting virus transport in porous media include advection, dispersion, attachment, detachment, and inactivation [e.g., *Matthess et al*., 1988; *Corapcioglu and Haridas*, 1984]. Attachment, or the association of viruses and other colloids with solid surfaces, has been modeled as colloid filtration [*Bales et al*., 1991, 1993; *Saiers et al*., 1994; *Johnson et al*., 1996], solute-like adsorption [*Tim and Mostaghimi*, 1991; *Park et al*., 1991], and a combination of equilibrium adsorption and filtration [*Jin et al*., 1997]. We chose to include both a kinetic adsorption-like term and colloid filtration as options for the attachment mechanism in our local-scale equations so that we could evaluate the sensitivity of the stochastic results to the spatial variability of each of these mechanisms. (As shown in the stochastic mean simulations presented later, we considered one or the other attachment mechanism but never both together. The two expressions for attachment are carried through the derivation for compactness of presentation.) Out of necessity such descriptions of virus attachment are oversimplified and do not adequately account for the fact that there is a whole spectrum of binding sites within a small volume of aquifer sediment, nor do they account for the fact that the makeup of binding sites is subject to spatial variability. The development of more accurate mathematical descriptions for colloidal attachment within aquifer sediments is beyond the scope of this paper.

The governing equations for transport of free and attached viruses are then given by

Local-scale transport of free viruses

$$\frac{\partial C}{\partial t} = \underbrace{-\frac{\partial}{\partial x_i}(v_i C)}_{\text{advection}} + \underbrace{\frac{\partial}{\partial x_i}\left(D_{ij}\frac{\partial C}{\partial x_j}\right)}_{\text{dispersion}} \underbrace{- k_{dc} C}_{\text{inactivation}}$$

$$\underbrace{- k_c C}_{\text{adsorption}} \underbrace{- \left[\frac{3}{2}\frac{(1-n)}{d}\alpha_c \eta\right] v_i C}_{\text{filtration}} + \underbrace{S\frac{1}{\rho}\frac{\rho_b}{n}k_y}_{\text{detachment}} \quad (1a)$$

Local-scale conservation of mass of attached viruses

$$\frac{\rho_b}{n}\frac{\partial S}{\partial t} = \underbrace{-k_{ds}\frac{\rho_b}{n}S}_{\text{inactivation}} + \underbrace{k_c \rho C}_{\text{adsorption}}$$

$$+ \underbrace{\left[\frac{3}{2}\frac{(1-n)}{d}\alpha_c \eta\right] v_i \rho C}_{\text{filtration}} - \underbrace{S\frac{\rho_b}{n}k_y}_{\text{detachment}} \quad (1b)$$

where C is the mass fraction of free viruses, S is the mass fraction of viruses attached to solid surfaces, v_i is the pore water velocity, D_{ij} is the local dispersion tensor, k_{dc} is the inactivation rate of free viruses, k_c is the virus adsorption coefficient, n is the effective porosity, d is d_{10}, the sieve size on which 90% of grains are retained, α_c is the collision efficiency factor, η is the single collector efficiency, ρ is the solution density, ρ_b is the bulk density of porous media, k_y is the virus detachment coefficient, and k_{ds} is the inactivation rate of attached viruses.

The local-scale coefficient of hydrodynamic dispersion for the free viruses is assumed to be of the following form [*Bear*, 1972], assuming that viruses may be assumed to behave like solutes for the purpose of determining local dispersivity:

$$D_{ij} = \alpha_T |v| \delta_{ij} + (\alpha_L - \alpha_T) v_i v_j / |v| + D_d^* \quad (2)$$

where α_L is the local longitudinal dispersivity, α_T is the local transverse dispersivity, $|v|$ is the magnitude of the pore water velocity, where $|v| = (v_1^2 + v_2^2 + v_3^2)^{1/2}$, v_i is the vector of the pore water velocity, δ_{ij} is the Kronecker delta function, and D_d^* is the porous media molecular diffusion coefficient.

2.2. Filtration and Bulk Density Parameterization in Terms of ln *K*

Colloid filtration is often defined in terms of two principal parameters: the collision efficiency factor (α_c), which represents the fraction of colloids that adhere to the soil grains after making contact, and the single collector efficiency (η), which represents the fraction of colloids in the fluid that come in contact with the grains. The mathematical expression derived by *Rajagopalan and Tien* [1976] was chosen to model η because (1) it is physically based, in that it accounts for the effect of neighboring grains on particle collection; (2) it has been previously used in modeling small-scale groundwater systems [e.g., *Martin et al*., 1992]; and (3) recent work has argued for its use over other models and has improved upon it in order to account for variable grain-size porous media [*Martin et al*., 1996; *Logan et al*., 1995].

In the *Rajagopalan and Tien* [1976] model, η is expressed as

$$\eta = \underbrace{4.0 A_s^{1/3}\left(\frac{3\pi\mu}{B_z T} n v_i d_p d\right)^{-2/3}}_{\text{diffusion}} + \underbrace{A_s\left(\frac{4H}{9\pi\mu}\right)^{1/8}\frac{d_p^{13/8}}{(n v_i)^{1/8} d^{15/8}}}_{\text{Van der Waal's forces and interception}}$$

$$+ \underbrace{0.00338 A_s\left[\frac{(\rho_p - \rho) g}{18\mu}\right]^{1.2}\frac{d_p^2 d^{0.4}}{(n v_i)^{1.2}}}_{\text{gravitational effects and interception}} \quad (3)$$

where d_p is the colloid diameter, H is the Hamaker constant, μ is dynamic viscosity, ρ_p is the buoyant density of the colloids, B_z is Boltzmann's constant, g is acceleration due to gravity, T is temperature, and A_s is $2[1 - (1-n)^{5/3}]/[2 - 3(1-n)^{1/3} + 3(1-n)^{5/3} - 2(1-n)^2]$. This complicated expression for η, incorporating filtration by diffusion, London or van der Waal's forces, gravity, and interception, is simplified in this work in order to more easily incorporate it into the stochastic model as follows.

The hydraulic conductivity variability is the independent input that drives the stochastic system. Because of the form of the governing flow equation [see *Rehmann*, 1998], it is convenient to consider the variability in the natural logarithm of hydraulic conductivity. A further benefit of this parameterization is that perturbations in the natural logarithm are smaller than perturbations in the hydraulic conductivity field itself, which is compatible with the small-perturbation assumption of the theoretical approach. In order to simplify the *Rajagopalan and Tien* [1976] model of single collector efficiency, the parameters of this model (porosity and effective grain size) are correlated with ln K by combining appropriate empirical expressions from the following sources: (1) published relations between both total porosity and specific yield and median grain diameter [*Davis and DeWiest*, 1966]; (2) laboratory column data relating median grain diameter to hydraulic conductivity [*Kauffman*, 1996]; (3) the assumption that specific yield provides a sufficient estimate of effective porosity [*Gorelick et al*., 1993; *U.S. Army Corps of Engineers*, 1982]; and (4) the *Hazen* [1911] relation between the d_{10} grain size and hydraulic conductivity. Making these substitutions [see *Rehmann*, 1998], the single collector efficiency expression then becomes a function of hydraulic conductivity and mean pore velocity, as well as other calculated constants such as colloid diameter, temperature, and colloid buoyant density. Hydraulic conductivity and velocity values are then varied over ranges observed in natural groundwater systems, and a system of planes is fit to the ln K-velocity-η^* system, where $\eta^* \equiv [3(1-n)/2d] v_i \eta$ (which can be incorporated directly into (1)). This system is expressed as

$$\eta^* \equiv \underbrace{a_{1P}(a_{10} + b_{10} v_i) e^{c_{10} \ln K}}_{\text{diffusion}} + \underbrace{a_{1L}(a_{11} + b_{11} v_i) e^{c_{11} \ln K}}_{\text{Van der Waal's forces and interception}}$$

$$+ \underbrace{a_{1G}(a_{12} + b_{12} v_i) e^{c_{12} \ln K}}_{\text{gravitational effects and interception}} \quad (4)$$

where (a_{10}, b_{10}, c_{10}), (a_{11}, b_{11}, c_{11}), and (a_{12}, b_{12}, c_{12}) are fitting constants, a_{1P} is $6 d_p^{-2/3}(3\pi\mu/B_z T)^{-2/3}$, a_{1L} is $1.5 d_p^{13/8}(4H/9\pi\mu)^{1/8}$, and a_{1G} is $(3/2)(0.00338) d_p^2 [(\rho_p - \rho) g/(18\mu)]^{1.2}$.

Each of the three components of (4) was fit independently, following the assumption in colloid filtration theory that these elements are additive. Figure 1 illustrates the two-step fitting

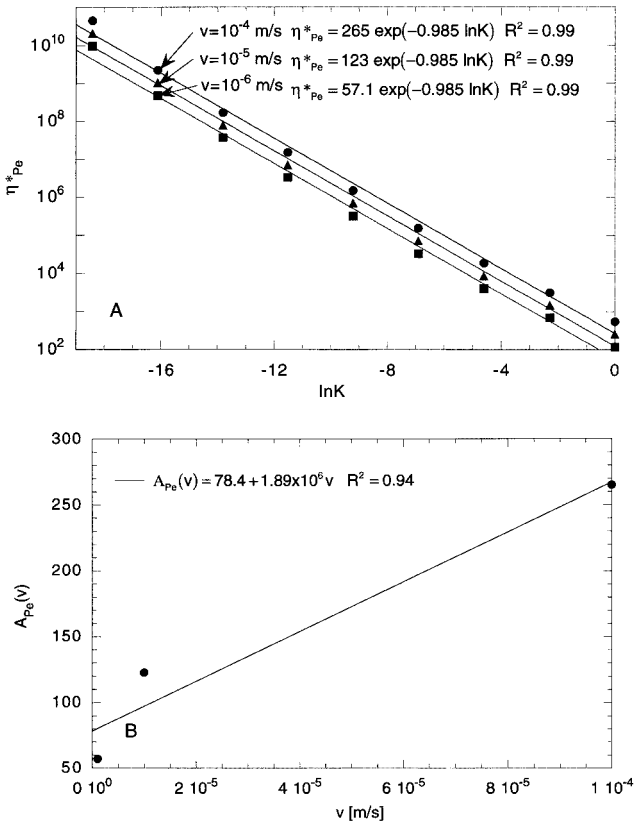

Figure 1. Two-step parameterization of η^* for the diffusion portion of filtration expression. (a) Fitting exponential functions to η^* versus ln K for different velocities, such that $\eta^* = A(v)$ exp $(c_{10} \ln K)$, and (b) fitting a line to $A(v)$ versus v.

of η^* for the first term (representing diffusion). For virus-size colloids, diffusion is the dominant mechanism governing transport to grain surfaces [*Bales et al*., 1991]. Figure 1a shows the first step of fitting to the $\eta^* - \ln K$ data for various mean pore velocities, giving an equation of the form $\eta^* = A(v)$ exp $(c_{10} \ln K)$. Figure 1b then shows the fitting of a line to $A(v) = a_{10} + b_{10}v$. Curve fits for the diffusion portion of η^* are very good, with R^2 values greater than 0.94 in both cases. Curve fits for the van der Waal's forces term ($R^2 = 0.99$ for both parameterization steps) were also excellent, while those for the gravity term ($R^2 = 0.96$ for the first parameterization step and 0.70 for the second parameterization step) were not as good, leading to poorer predictions of the transport of larger colloids (1–10 μm diameter).

The colloid filtration model of *Rajagopalan and Tien* [1976] was originally developed to simulate particle removal in a deep-bed filters. Deep-bed filters differ significantly from natural sediments in that their characteristic pore water velocities are usually much greater than that those typically associated with aquifer flow (e.g., 100 m d^{-1} versus 1 m d^{-1}), and deep-bed filters are typically composed of a much smaller range of grain sizes than natural soils. *Martin et al*. [1996] found that, using the *Rajagopalan and Tien* [1976] single collector efficiency expression, the d_{10} of a volume distribution of grain sizes most accurately described bacterial transport in sorted porous media. We therefore incorporated the use of d_{10} into our analysis since it aligns the single collector efficiency expression of Rajagopalan and Tien more closely to that of a heterogeneous sediment.

Using a similar parameterization, the recurring ρ_b/n group is also expressed in terms of ln K, where

$$\rho_b/n = \rho_s a_r e^{b_r \ln K} \tag{5}$$

$\rho_b = \rho_s(1 - n_b)$, ρ_s is the soil grain density, n_b is total porosity, and a_r and b_r are fitting parameters.

2.3. Correlation of Virus Parameters With Soil Type

Virus attachment and detachment parameters are taken as being correlated with soil type as represented by ln K, leading to attachment and detachment random variables driven by variability in ln K. The effects of solution (e.g., pH and ionic strength) and variable virus properties (e.g., surface properties, size, and shape) on attachment and detachment are not considered directly and are beyond the scope of this paper. However, it is important to note that the collision efficiency factor (α_c) can be very sensitive to solution properties, virus type, and soil properties unrelated to ln K. Laboratory experiments have shown, for example, that bacteriophages MS2 and PRD-1, although similar in size, differ significantly in their transport behavior due to differences in structural architecture [*Redman et al*., 1997; *Penrod et al*., 1996]. Therefore the attachment and detachment coefficients are not expected to be completely correlated to ln K, and the uncorrelated portion can account for some of this nonporous media related variability. The main objective, however, is achieved, as spatial variability in α_c and other attachment and detachment parameters is incorporated and is expected to exist. Unlike the porosity and grain size terms present in η and ρ_b/n, there are no established empirical expressions relating virus attachment and detachment parameters to ln K. Therefore, using the approach of *Garabedian et al*. [1988], we postulate that

$$k_c = a_1 + b_1 \ln K + \delta_1 \tag{6}$$

where a_1 and b_1 are constants and δ_1 represents random portion of the adsorption coefficient that cannot be accounted for by variability in the ln K field. Using this approach, it is therefore possible for the adsorption coefficient k_c to be positively correlated to ln $K(b_1 > 0)$, negatively correlated to ln $K(b_1 < 0)$, or uncorrelated to ln $K(b_1 = 0)$.

Similar expressions are used to describe both the detachment and collision efficiency parameters:

$$k_y = a_2 + b_2 \ln K + \delta_2 \tag{7}$$

$$\alpha_c = a_3 + b_3 \ln K + \delta_3 \tag{8}$$

Although (6) through (8) are simple linear relations, their objective is to capture the general trend of virus attachment and detachment parameters observed experimentally. Numerical values for a_i, b_i, and δ_i $(i = 1, 2, 3)$ are not readily available, but an example set of values can be determined in the laboratory. Several researchers have observed that soils characterized by different hydraulic conductivity values have dissimilar colloid attachment and detachment rates. For example, *Morley et al*. [1998] measured bacterial attachment and detachment rates in a high-conductivity and a low-conductivity soil and found that the fitted attachment rate was highest in the low-conductivity material, while the fitted detachment rate was greatest in the higher conductivity material. *Harvey et al*. [1993]

hypothesized that the late arrival of colloids (bacteria and microspheres) in small field tests might be due to the presence of iron-rich coatings, minerals which are most abundant in the finer-grained sediments in the Cape Cod aquifer, leading to greater colloid attachment. For the simulations performed in this paper, detachment is assumed to be uncorrelated with ln K ($b_2 = 0$) in order to focus on attachment effects.

Although there is little evidence in the literature for correlation of virus inactivation with soil type [e.g., *Sobsey et al.*, 1980, 1986], it is expected that there will be some variability in the virus inactivation rate in the aquifer. Therefore inactivation of both free and attached viruses are considered to be correlated with ln K in this work, as represented by

$$k_{dc} = a_4 + b_4 \ln K + \delta_4 \tag{9}$$

$$k_{ds} = a_5 + b_5 \ln K + \delta_5 \tag{10}$$

where a_i, b_i, and δ_i are defined similarly to (6)–(8). While (9) and (10) were used in the derivation of the stochastic model to make it as general as possible, in all subsequent simulations conducted for this paper it was assumed that inactivation was not correlated with the ln K field, that is, $b_4 = b_5 = 0$. If new evidence is found demonstrating that virus inactivation rate is correlated (either positively or negatively) with porous media type, such relations could be easily incorporated into the model through the specification of nonzero values of b_4 and b_5 in the stochastic results.

2.4. Random Field Representation

The stochastic analytical approach [*Lumley and Panofsky*, 1964; *Gelhar*, 1993] used here assumes that the observed three-dimensional variation in hydraulic conductivity of an aquifer can be modeled as a second-order stationary, correlated random field, where the variability of the porous medium is characterized by statistical parameters rather than by a point-by-point description. The ln K variability is assumed to drive variability in other quantities, including physical aquifer parameters such as effective porosity, as well as virus transport parameters such as collision efficiency. The three-dimensional random field representation for the ln K field is given as

$$\ln K(\mathbf{x}) = f(\mathbf{x}) = \bar{f} + f'(\mathbf{x}) \tag{11}$$

where $\mathbf{x} = (x_1, x_2, x_3)$ is the vector of spatial coordinates and the overbar and prime denote mean and perturbation quantities, respectively. This statistically homogeneous (stationary) process may be characterized by its covariance function

$$R_{ff}(\boldsymbol{\xi}) = E[f'(\boldsymbol{\xi} + \mathbf{x}) f'(\mathbf{x})] \tag{12}$$

which depends only on the separation vector $\boldsymbol{\xi}$, where $E[\ \ ]$ is the expected value operator.

A particular form of (12) which has been shown to adequately represent field data [*Hess et al.*, 1992] is the negative-exponential covariance function, which is given by

$$R_{ff}(\boldsymbol{\xi}) = \sigma_f^2 \exp\left[-(\xi_1^2/\lambda_1^2 + \xi_2^2/\lambda_2^2 + \xi_3^2/\lambda_3^2)^{1/2}\right] \tag{13}$$

where σ_f^2 is the variance of the ln K field and λ_i represents the correlation scale in the x_i direction. This covariance function has as its corresponding spectrum

$$S_{ff}(\mathbf{k}) = \sigma_f^2 \lambda_1 \lambda_2 \lambda_3 / [\pi^2 (1 + \lambda_1^2 k_1^2 + \lambda_2^2 k_2^2 + \lambda_3^2 k_3^2)^2] \tag{14}$$

where $\mathbf{k} = (k_1, k_2, k_3)$ is the wave number vector. Equations (13) and (14) imply modeling of a heterogeneous, anisotropic ln K random field. This form was chosen (as opposed to the simpler isotropic form) since most natural materials are somewhat anisotropic, at least in the vertical compared to the horizontal (i.e., $\lambda_1 = \lambda_2 \neq \lambda_3$). This parameterization allows assessment of the effect of sediment stratification on mean virus transport.

Because hydraulic conductivity controls the flow and transport processes in porous media, the dependent variables (free and attached virus concentrations and pore water velocity) will also vary in a way that can be characterized statistically. These variables, in addition to coefficients that depend on them or on ln K, can also be expressed as three-dimensional random fields. Each can be defined as the sum of a mean and perturbation as follows:

$$C(\mathbf{x}, t) = \bar{c}(\mathbf{x}, t) + c'(\mathbf{x}, t) \tag{15a}$$

$$S(\mathbf{x}, t) = \bar{s}(\mathbf{x}, t) + s'(\mathbf{x}, t) \tag{15b}$$

$$v_i(\mathbf{x}) = \bar{v}_i(\mathbf{x}) + v_i'(\mathbf{x}) \tag{15c}$$

$$\frac{\rho_b}{n}(\mathbf{x}) = r(\mathbf{x}) = \bar{r} + r'(\mathbf{x}) \tag{15d}$$

$$\eta^*(\mathbf{x}) = \bar{\eta}^*(\mathbf{x}) + \eta^{*\prime}(\mathbf{x}) \tag{15e}$$

$$k_c(\mathbf{x}) = \bar{k}_c + k_c'(\mathbf{x}) \tag{15f}$$

$$k_y(\mathbf{x}) = \bar{k}_y + k_y'(\mathbf{x}) \tag{15g}$$

$$\alpha_c(\mathbf{x}) = \bar{\alpha}_c + \alpha_c'(\mathbf{x}) \tag{15h}$$

$$k_{dc}(\mathbf{x}) = \bar{k}_{dc} + k_{dc}'(\mathbf{x}) \tag{15i}$$

$$k_{ds}(\mathbf{x}) = \bar{k}_{ds} + k_{ds}'(\mathbf{x}) \tag{15j}$$

where the overbar and prime represent the mean and perturbation, respectively, and the variable names are defined previously. For the general linear relations presented as (6) through (10), the mean and perturbation may be expressed as $(a_i + b_i\bar{f})$ and $(b_i f' + \delta_i)$, respectively, and perturbations in ρ_b/n and η^* are completely correlated with ln K. All random fields given in (15) are by definition a function of space; in addition, the concentrations of free and attached viruses are dependent on time when the transient problem is solved. Here δ_i ($i = 1, \cdots, 5$) are zero-mean random fields uncorrelated to the ln K field and are assumed to be characterized by negative exponential covariance functions. The spectra for δ_i are therefore of the same form as (14), with the exception that their variances ($\sigma_{\delta_i}^2$) and correlation scales (λ_{1_i}, λ_{2_i}, λ_{3_i}) may differ from that of the ln K covariance function.

2.5. Derivation of Mean and Perturbation Equations

Mean conservation equations for free and attached viruses can be obtained by substituting the random field representations given in (6) through (10) and (15) into the local equations (1a) and (1b) and taking the expected value of result to yield

Mean equation for transport of free viruses

$$\frac{\partial \bar{c}}{\partial t} - v_e \frac{\partial \bar{c}}{\partial \zeta_1} = \left\{ -\left(\bar{v} \frac{\partial \bar{c}}{\partial \zeta_1} + \frac{\partial \overline{v_i' c'}}{\partial \zeta_i} \right) + \frac{\partial}{\partial \zeta_i} \left(D_{ij} \frac{\partial \bar{c}}{\partial \zeta_j} \right) \right.$$
$$- \bar{c}(\bar{k}_{dc} + \bar{k}_c + \bar{\alpha}_c \eta_0) + \frac{\bar{r}}{\rho} \bar{k}_y \bar{s} - \overline{v_i' c'} \bar{\alpha}_c \eta_2$$
$$- \overline{f' c'}(b_1 + b_3 \eta_0 + b_4 + \bar{\alpha}_c \eta_1)$$
$$+ \overline{f' s'} \frac{\bar{r}}{\rho} \left(\bar{k}_y \frac{\rho_s a_r b_r K_g^{b_r}}{\bar{r}} + b_2 \right)$$
$$- \overline{f' v_i'} \bar{c}(b_3 \eta_2 + \bar{\alpha}_c \eta_4) + \overline{f'^2}[-\bar{c}(b_3 \eta_1 + \bar{\alpha}_c \eta_3)$$
$$\left. + \bar{s} \rho^{-1} b_2 \rho_s a_r b_r K_g^{b_r}] - (\overline{c' \delta_1'} + \overline{c' \delta_3'} \eta_0 + \overline{c' \delta_4'}) + \frac{\bar{r}}{\rho} \overline{s' \delta_2'} \right\} \tag{16a}$$

Mean equation for conservation of mass of attached viruses

$$\frac{\partial \bar{s}}{\partial t} + \overline{f' \frac{\partial s'}{\partial t}} \frac{\rho_s a_r b_r K_g^{b_r}}{\bar{r}} = \left\{ -\bar{s}(\bar{k}_{ds} + \bar{k}_y) + \bar{c} \frac{\rho}{\bar{r}} (\bar{k}_c + \bar{\alpha}_c \eta_0) \right.$$
$$- \overline{f' s'} \left([b_2 + b_5] + \frac{\rho_s a_r b_r K_g^{b_r}}{\bar{r}} [\bar{k}_{ds} + \bar{k}_y] \right)$$
$$+ \overline{f'^2} \left(-\bar{s} \frac{\rho_s a_r b_r K_g^{b_r}}{\bar{r}} [b_2 + b_5] + \bar{c} \frac{\rho}{\bar{r}} [b_3 \eta_1 + \bar{\alpha}_c \eta_3] \right) \tag{16b}$$
$$+ \overline{f' v_i'} \bar{c} \frac{\rho}{\bar{r}} (b_3 \eta_2 + \bar{\alpha}_c \eta_4) + \overline{f' c'} \frac{\rho}{\bar{r}} (b_1 + \bar{\alpha}_c \eta_1 + b_3 \eta_0)$$
$$\left. + \frac{\rho}{\bar{r}} \overline{v_i' c'} \bar{\alpha}_c \eta_2 + \frac{\rho}{\bar{r}} (\overline{c' \delta_1'} + \overline{c' \delta_3'} \eta_0) - (\overline{s' \delta_2'} + \overline{s' \delta_5'}) \right\}$$

The following manipulations were used to derive the form of (16): (1) The x_1 axis is aligned with the mean flow direction such that $\bar{v}_1 = \bar{v}$, $\bar{v}_2 = \bar{v}_3 = 0$, and therefore the local dispersion tensor can be approximated in the form of *Naff* [1978] as $D_{11} = \alpha_L \bar{v}$, $D_{22} = D_{33} = \alpha_T \bar{v}$, $D_{ij} = 0$ for $i \neq j$. (2) A moving coordinate system [*Miralles-Willhelm and Gelhar*, 1996b; *Rehmann*, 1998, appendix B] has been invoked in which

$$\zeta_1 = x_1 - \int_0^t v_e \, dt' \qquad \zeta_2 = x_2 \qquad \zeta_3 = x_3$$

and v_e is the unknown effective free-virus velocity. (3) The substitution $e^{\bar{f}} = K_g$ has been made. (4) The exponential functions of perturbations have been expanded in series form ($e^{f'} = 1 + f' + f'^2/2 + \dots$). (5) The colloid filtration parameter η^* has been expanded to give $\eta^* \equiv (\eta_0 + f' \eta_1 + v_i' \eta_2 + f'^2 \eta_3 + f' v_i' \eta_4 + \dots)$, where η_0 is $[K_g^{c10}(a_{10} + b_{10}\bar{v}) + K_g^{c11}(a_{11} + b_{11}\bar{v}) + K_g^{c12}(a_{12} + b_{12}\bar{v})]$, η_1 is $[K_g^{c10} c_{10}(a_{10} + b_{10}\bar{v}) + K_g^{c11} c_{11}(a_{11} + b_{11}\bar{v}) + K_g^{c12} c_{12}(a_{12} + b_{12}\bar{v})]$, η_2 is $[K_g^{c10} b_{10} + K_g^{c11} b_{11} + K_g^{c12} b_{12}]$, η_3 is $(1/2)[K_g^{c10} c_{10}^2(a_{10} + b_{10}\bar{v}) + K_g^{c11} c_{11}^2(a_{11} + b_{11}\bar{v}) + K_g^{c12} c_{12}^2(a_{12} + b_{12}\bar{v})]$, and η_4 is $[K_g^{c10} b_{10} c_{10} + K_g^{c11} b_{11} c_{11} + K_g^{c12} b_{12} c_{12}]$.

The mean virus conservation equations (16) include cross-perturbation terms (e.g., $\overline{f' c'}$) that are not present in the local-scale equations. These macroscopic terms result from the averaging process and represent the effect of spatial variability on virus transport. The first-order perturbation equations necessary to evaluate these cross-perturbation terms are obtained by subtracting the mean equations (16) from the original random-field-substituted equations ((6)–(10) and (15) substituted into (1a) and (1b)), assuming that products of small perturbations can be approximated by the products of their means and are expressed as

First-order perturbation equation for transport of free viruses

$$\frac{\partial c'}{\partial t} = \left\{ -(\bar{v} - v_e) \frac{\partial c'}{\partial \zeta_1} + \frac{\partial}{\partial \zeta_i} \left(D_{ij} \frac{\partial c'}{\partial \zeta_j} \right) \right.$$
$$- c'(\bar{k}_{dc} + \bar{k}_c + \bar{\alpha}_c \eta_0) + \frac{\bar{r}}{\rho} \bar{k}_y s'$$
$$+ f' \left[-\bar{c}(b_1 + b_3 \eta_0 + b_4 + \bar{\alpha}_c \eta_1) \right. \tag{17a}$$
$$\left. \left. + \bar{s} \frac{\bar{r}}{\rho} \left(\bar{k}_y \frac{\rho_s a_r b_r K_g^{b_r}}{\bar{r}} + b_2 \right) \right] - v_i' \left(\bar{c} \bar{\alpha}_c \eta_2 + \frac{\partial \bar{c}}{\partial \zeta_i} \right) \right.$$
$$\left. - \bar{c}(\delta_1' + \delta_3' \eta_0 + \delta_4') + \frac{\bar{r}}{\rho} \bar{s} \delta_2' \right\}$$

First-order perturbation equation for conservation of mass of attached viruses

$$\frac{\partial s'}{\partial t} + f' \frac{\partial \bar{s}}{\partial t} \frac{\rho_s a_r b_r K_g^{b_r}}{\bar{r}} = \left\{ -s'(\bar{k}_{ds} + \bar{k}_y) + \frac{\rho}{\bar{r}} c'(\bar{k}_c + \bar{\alpha}_c \eta_0) \right.$$
$$+ \bar{c} \frac{\rho}{\bar{r}} (v_i' \bar{\alpha}_c \eta_2 + \delta_1' + \delta_3' \eta_0) - \bar{s}(\delta_2' + \delta_5')$$
$$+ f' \left[-\bar{s} \left(\frac{\rho_s a_r b_r K_g^{b_r}}{\bar{r}} [\bar{k}_{ds} + \bar{k}_y] + [b_2 + b_5] \right) \right. \tag{17b}$$
$$\left. \left. + \frac{\rho}{\bar{r}} \bar{c}(b_1 + \bar{\alpha}_c \eta_1 + b_3 \eta_0) \right] \right\}$$

This method of truncation theoretically restricts the application of the small perturbation results to mildly heterogeneous porous media, that is, $\sigma_f^2 \ll 1$. This restriction has been highlighted in the literature for a number of years (see, for example, recent reviews by *Gelhar* [1997, p. 162] and *Neuman* [1997, p. 238]). For transport of a conservative tracer in isotropic porous media, comparison of stochastic results to Monte Carlo simulations [see *Gelhar and Axness*, 1983, Figure 10] and single-realization simulations [*Tompson and Gelhar*, 1990; *Jussel et al.*, 1990] have shown that the stochastic results appear to be robust for $\sigma_f^2 < 2$, which is a surprisingly high degree of heterogeneity given the theoretical restrictions of the approach. Although the virus transport results should likewise be theoretically restricted to being applicable to only very small values of σ_f^2 (i.e., $\sigma_f^2 \ll 1$), it is not known to what degree this theoretical restriction can be violated, but on the basis of other small perturbation results it is unlikely that the approach will be applicable to highly heterogeneous aquifers ($\sigma_f^2 \gg 1$). This conjecture can be evaluated by comparison of the theory with appropriately designed Monte Carlo or single-realization simulations, which is a planned next step of our work on this topic.

2.6. Evaluation of Cross-Perturbation Terms

Assuming local statistical homogeneity, the Fourier-Stieltjes representations of the perturbation terms are given by

$$f'(\mathbf{x}) = \int_{-\infty}^{\infty} \int \int e^{i(\mathbf{k} \cdot \mathbf{x})} \, dZ_f(\mathbf{k}) \tag{18a}$$

$$v_i'(\mathbf{x}) = \int_{-\infty}^{\infty}\int\int e^{i(\mathbf{k}\cdot\mathbf{x})}\, dZ_{v_i}(\mathbf{k}) \tag{18b}$$

$$c'(\mathbf{x}, t) = \int_{-\infty}^{\infty}\int\int e^{i(\mathbf{k}\cdot\mathbf{x})}\, dZ_c(\mathbf{k}, t) \tag{18c}$$

$$s'(\mathbf{x}, t) = \int_{-\infty}^{\infty}\int\int e^{i(\mathbf{k}\cdot\mathbf{x})}\, dZ_s(\mathbf{k}, t) \tag{18d}$$

$$\delta_i(\mathbf{x}) = \int_{-\infty}^{\infty}\int\int e^{i(\mathbf{k}\cdot\mathbf{x})}\, dZ_{\delta_i}(\mathbf{k}) \qquad i = 1, \ldots, 5 \tag{18e}$$

where, for example, $dZ_f(\mathbf{k})$ is the Fourier-Stieltjes amplitude of the $f'(\mathbf{x})$ field and the corresponding spectrum is defined as $S_{ff}(\mathbf{k})d\mathbf{k} = E[dZ_f(\mathbf{k})dZ_f^*(\mathbf{k})]$ (the asterisk denotes the complex conjugate) [*Lumley and Panofsky*, 1964].

Substituting (18a) through (18e) into the perturbation equations (17a) and (17b) and by uniqueness of the spectral representation [*Lumley and Panofsky*, 1964], the Fourier-Stieltjes amplitude for virus concentration can be expressed in terms of the Fourier-Stieltjes amplitudes of ln K and other random fields as follows:

Fourier-Stieltjes amplitude equation for transport of free viruses

$$\begin{aligned}\frac{\partial dZ_c(\mathbf{k}, t)}{\partial t} &= \left\{ -dZ_c(\mathbf{k}, t)\left(ik_1\bar{v} + k_ik_jD_{ij} + [\bar{k}_{dc} + \bar{k}_c + \bar{\alpha}_c\eta_0]\right)\right.\\ &\quad + \frac{\bar{r}}{\rho}\, dZ_s(\mathbf{k}, t)\bar{k}_y + dZ_f(\mathbf{k})\left[-\bar{c}(b_1 + b_3\eta_0 + b_4 + \bar{\alpha}_c\eta_1)\right.\\ &\quad \left. + \bar{s}\,\frac{\bar{r}}{\rho}\left(\bar{k}_y\,\frac{\rho_s a_r b_r K_g^{b_r}}{\bar{r}} + b_2\right)\right] - dZ_{v_i}(\mathbf{k})\left(\frac{\partial\bar{c}}{\partial\zeta_i} + \bar{c}\,\bar{\alpha}_c\eta_2\right)\\ &\quad \left. - \bar{c}(dZ_{\delta_1}(\mathbf{k}) + \eta_0 dZ_{\delta_3}(\mathbf{k}) + dZ_{\delta_4}(\mathbf{k})) + \frac{\bar{r}}{\rho}\,\bar{s}dZ_{\delta_2}(\mathbf{k})\right\}\end{aligned} \tag{19a}$$

Fourier-Stieltjes amplitude equation for conservation of mass of attached viruses

$$\begin{aligned}\frac{\partial dZ_s(\mathbf{k}, t)}{\partial t} &= \left\{ -dZ_s(\mathbf{k}, t)(\bar{k}_{ds} + \bar{k}_y) + dZ_c(\mathbf{k}, t)\,\frac{\rho}{\bar{r}}\,(\bar{k}_c + \bar{\alpha}_c\eta_0)\right.\\ &\quad + dZ_f(\mathbf{k})\left[-\frac{\partial\bar{s}}{\partial t}\,\frac{\rho_s a_r b_r K_g^{b_r}}{\bar{r}} + \bar{c}\,\frac{\rho}{\bar{r}}\,(b_1 + \bar{\alpha}_c\eta_1 + b_3\eta_0)\right.\\ &\quad \left. - \bar{s}\left(\frac{\rho_s a_r b_r K_g^{b_r}}{\bar{r}}\,(\bar{k}_{ds} + \bar{k}_y) + (b_2 + b_5)\right)\right]\\ &\quad + \bar{c}\,\frac{\rho}{\bar{r}}\,(dZ_{v_i}(\mathbf{k})\bar{\alpha}_c\eta_2 + dZ_{\delta_1}(\mathbf{k}) + dZ_{\delta_3}(\mathbf{k})\eta_0)\\ &\quad \left. - \bar{s}(dZ_{\delta_2}(\mathbf{k}) + dZ_{\delta_5}(\mathbf{k}))\right\}\end{aligned} \tag{19b}$$

In order to solve this system of equations for $dZ_c(\mathbf{k})$ and $dZ_s(\mathbf{k})$, it is necessary to perform an intermediate step involving a time scaling of the concentration perturbation amplitudes [*Miralles-Wilhelm and Gelhar*, 1996a, b; *Rehmann*, 1998]. Because the total masses of free and attached viruses vary in time owing to attachment (adsorption and filtration), detachment, and inactivation, changes in time of mean concentrations, concentration perturbations, and mean gradients cannot be neglected as they are for a conservative solute. For the conservative case these quantities can be considered relatively constant, leading to a simple solution to the Fourier-Stieltjes amplitude expression using the approximation of *Gelhar* [1987]. This approximation uses the fact that the integral to be solved is composed of exponentially weighted functions of time which can be expanded in a Taylor series about a single point in time. To solve the Fourier-Stieltjes amplitude expressions for free and attached viruses (equations (19a) and (19b)), it is necessary to follow the plumes of free and attached viruses in time to effectively remove these changes in concentration due to attachment, detachment, and inactivation. In this new reference frame, advection and dispersion are separated from other effects, allowing solution of the system of equations using the Taylor series expansion approximation.

Considering attachment, detachment, and inactivation to be the cause of temporal changes in the concentration perturbation amplitudes ($dZ_c(\mathbf{k})$ and $dZ_s(\mathbf{k})$), a simplified system of equations is solved as an intermediate step (appendix A). Solution of the simplified system introduces concentration perturbation amplitudes for the conservative case (advection and dispersion only), $dZ_{\hat{c}}(\mathbf{k})$ and $dZ_{\hat{s}}(\mathbf{k})$, by incorporating the initial condition $dZ_c(\mathbf{k}) = dZ_{\hat{c}}(\mathbf{k})$ and $dZ_s(\mathbf{k}) = dZ_{\hat{s}}(\mathbf{k})$ at time = 0. When the perturbation equations are expressed in terms of these conservative quantities, the system of equations is solved using the approximation of *Gelhar* [1987] described above. Finally, these expressions are transformed to yield equations for the original concentration perturbation amplitudes:

Simplified Fourier-Stieltjes amplitude equation for transport of free viruses

$$\begin{aligned}dZ_c(\mathbf{x}, t) = \frac{1 - e^{-\beta^* t}}{\beta^*}&\left\{ dZ_f\left(-\bar{c}[\bar{\alpha}_c\eta_1 + b_1 + b_3\eta_0 + b_4]\right.\right.\\ &\left. + \bar{s}\,\frac{\bar{r}}{\rho}\left[\bar{k}_y\,\frac{\rho_s a_r b_r K_g^{b_r}}{\bar{r}} + b_2\right]\right) + dZ_{v_i}(G_i - \bar{c}\,\bar{\alpha}_c\eta_2)\\ &\left. - \bar{c}(dZ_{\delta_1} + dZ_{\delta_3}\eta_0 + dZ_{\delta_4}) + \frac{\bar{r}}{\rho}\,dZ_{\delta_2}\bar{s}\right\}\end{aligned} \tag{20a}$$

Simplified Fourier-Stieltjes amplitude equation for conservation of mass of attached viruses

$$\begin{aligned}dZ_s(\mathbf{x}, t) = \frac{1 - e^{-\beta^* t}}{\beta^*}&\left\{ dZ_f\left[\frac{\rho}{\bar{r}}\,\bar{c}(\bar{\alpha}_c\eta_1 + b_1 + b_3\eta_0)\right.\right.\\ &\left. - \frac{\partial\bar{s}}{\partial t}\,\frac{\rho_s a_r b_r K_g^{b_r}}{\bar{r}} - \bar{s}\left((\bar{k}_{ds} + \bar{k}_y)\,\frac{\rho_s a_r b_r K_g^{b_r}}{\bar{r}} + b_2 + b_5\right)\right]\\ &\left. + \frac{\rho}{\bar{r}}\,\bar{c}(dZ_{v_i}\bar{\alpha}_c\eta_2 + dZ_{\delta_1} + dZ_{\delta_3}\eta_0) - \bar{s}(dZ_{\delta_2} + dZ_{\delta_5})\right\}\end{aligned} \tag{20b}$$

where $G_i = -\partial\bar{c}/\partial\zeta_i$ and $\beta^* = [ik_1\bar{v} + k_ik_jD_{ij} + ((\bar{k}_c + \bar{\alpha}_c\eta_0 + \bar{k}_{dc}) + \alpha_1)] + [(\bar{k}_y + \bar{k}_{ds}) + \beta_2]$. Parameters α_1 and β_2 are unknown effective loss coefficients for free and attached viruses, respectively, which differ from the mean loss rates and were introduced in the intermediate time-transformation step. These final expressions are used to evaluate the cross-perturbation terms in the mean equations (16a) and (16b).

In order to evaluate the products of perturbations appearing in the mean equations, the appropriate cross spectra must be evaluated. From (16a) and (16b), noting that $\overline{f'^2} = \sigma_f^2$, the cross terms to be evaluated are

$$\overline{f'v_i'} = \int_{-\infty}^{\infty}\int\int S_{fv_i}(\mathbf{k})\,d\mathbf{k} = \frac{\bar{v}}{\gamma}\int_{-\infty}^{\infty}\int\int S_{ff}(\mathbf{k})\,d\mathbf{k} \tag{21}$$

$$\overline{f'c'} = \int_{-\infty}^{\infty}\int\int S_{fc}(\mathbf{k})\,d\mathbf{k} = \left\{\left[-\bar{c}(\bar{\alpha}_c\eta_1 + b_1 + b_3\eta_0 + b_4) + \bar{s}\,\frac{\bar{r}}{\rho}\left(\bar{k}_y\,\frac{\rho_s a_r b_r K_g^{b_r}}{\bar{r}} + b_2\right)\right]\int_{-\infty}^{\infty}\int\int \frac{1-e^{-\beta^* t}}{\beta^*} S_{ff}(\mathbf{k})\,d\mathbf{k} + (G_j - \bar{c}\,\bar{\alpha}_c\eta_2)\int_{-\infty}^{\infty}\int\int \frac{1-e^{-\beta^* t}}{\beta^*} S_{fv_j}(\mathbf{k})\,d\mathbf{k}\right\} \tag{22}$$

$$\overline{v_i'c'} = \int_{-\infty}^{\infty}\int\int S_{v_ic}(\mathbf{k})\,d\mathbf{k} = \left\{\left[-\bar{c}(\bar{\alpha}_c\eta_1 + b_1 + b_3\eta_0 + b_4) + \bar{s}\,\frac{\bar{r}}{\rho}\left(\bar{k}_y\,\frac{\rho_s a_r b_r K_g^{b_r}}{\bar{r}} + b_2\right)\right]\int_{-\infty}^{\infty}\int\int \frac{1-e^{-\beta^* t}}{\beta^*} S_{fv_i}(\mathbf{k})\,d\mathbf{k} + (G_j - \bar{c}\,\bar{\alpha}_c\eta_2)\int_{-\infty}^{\infty}\int\int \frac{1-e^{-\beta^* t}}{\beta^*} S_{v_iv_j}(\mathbf{k})\,d\mathbf{k}\right\} \tag{23}$$

$$\overline{f's'} = \int_{-\infty}^{\infty}\int\int S_{fs}(\mathbf{k})\,d\mathbf{k} = \left\{\left[\bar{c}\,\frac{\rho}{\bar{r}}\,(\bar{\alpha}_c\eta_1 + b_1 + b_3\eta_0) - \frac{\partial\bar{s}}{\partial t}\,\frac{\rho_s a_r b_r K_g^{b_r}}{\bar{r}} - \bar{s}\left((\bar{k}_{ds} + \bar{k}_y)\,\frac{\rho_s a_r b_r K_g^{b_r}}{\bar{r}} + (b_2 + b_5)\right)\right]\cdot\int_{-\infty}^{\infty}\int\int \frac{1-e^{-\beta^* t}}{\beta^*} S_{ff}(\mathbf{k})\,d\mathbf{k} + \frac{\rho}{\bar{r}}\,\bar{c}\,\bar{\alpha}_c\eta_2\cdot\int_{-\infty}^{\infty}\int\int \frac{1-e^{-\beta^* t}}{\beta^*} S_{fv_j}(\mathbf{k})\,d\mathbf{k}\right\} \tag{24}$$

$$\overline{c'\delta_1'} = \int_{-\infty}^{\infty}\int\int S_{c\delta_1}(\mathbf{k})\,d\mathbf{k} = -\bar{c}\int_{-\infty}^{\infty}\int\int \frac{1-e^{-\beta^* t}}{\beta^*} S_{\delta_1\delta_1}(\mathbf{k})\,d\mathbf{k} \tag{25}$$

$$\overline{s'\delta_2'} = \int_{-\infty}^{\infty}\int\int S_{s\delta_2}(\mathbf{k})\,d\mathbf{k} = -\bar{s}\int_{-\infty}^{\infty}\int\int \frac{1-e^{-\beta^* t}}{\beta^*} S_{\delta_2\delta_2}(\mathbf{k})\,d\mathbf{k} \tag{26}$$

$$\overline{c'\delta_3'} = \int_{-\infty}^{\infty}\int\int S_{c\delta_3}(\mathbf{k})\,d\mathbf{k} = -\bar{c}\,\eta_0\cdot\int_{-\infty}^{\infty}\int\int \frac{1-e^{-\beta^* t}}{\beta^*} S_{\delta_3\delta_3}(\mathbf{k})\,d\mathbf{k} \tag{27}$$

$$\overline{c'\delta_4'} = \int_{-\infty}^{\infty}\int\int S_{c\delta_4}(\mathbf{k})\,d\mathbf{k} = -\bar{c}\int_{-\infty}^{\infty}\int\int \frac{1-e^{-\beta^* t}}{\beta^*} S_{\delta_4\delta_4}(\mathbf{k})\,d\mathbf{k} \tag{28}$$

$$\overline{s'\delta_5'} = \int_{-\infty}^{\infty}\int\int S_{c\delta_5}(\mathbf{k})\,d\mathbf{k} = -\bar{s}\int_{-\infty}^{\infty}\int\int \frac{1-e^{-\beta^* t}}{\beta^*} S_{\delta_5\delta_5}(\mathbf{k})\,d\mathbf{k} \tag{29}$$

Evaluating these integrals (see appendix B) for the case of a highly stratified aquifer (i.e., $\lambda_1 = \lambda_2 \gg \lambda_3$) [*Gelhar and Axness*, 1983], substituting the results into the mean equations (16), and returning to the original coordinate system, the resultant mean field-scale free-virus transport and attached-virus conservation equations are given by [*Rehmann*, 1998]

Final mean equation for transport of free viruses

$$\frac{\partial\bar{c}}{\partial t} + \underline{\underline{\frac{\partial\bar{s}}{\partial t}\,\frac{\bar{r}}{\rho}\,I_{1_{ij}}QR}} = \left\{-\underline{v_e}\,\frac{\partial\bar{c}}{\partial x_1} + D_{ij}\,\frac{\partial^2\bar{c}}{\partial x_i\partial x_j} + \underline{\underline{\left(\frac{\bar{v}^2}{\gamma^2}\,I_{1_{ij}}\right)\frac{\partial^2\bar{c}}{\partial x_1^2}}} + \frac{\bar{r}}{\rho}\,(\bar{k}_y + \underline{\underline{A_x}})\bar{s} - ([\bar{k}_{dc} + \bar{k}_c + \bar{\alpha}_c\eta_0] + \underline{\underline{A_c}})\bar{c} - \underline{\underline{\frac{\partial\bar{s}}{\partial x_1}\,\frac{\bar{r}}{\rho}\left(\frac{\bar{v}}{\gamma} + v_eR\right)I_{1_{ij}}Q}}\right\} \tag{30a}$$

Final mean equation for conservation of mass of attached viruses

$$\frac{\partial\bar{s}}{\partial t} - \underline{\underline{\frac{\partial^2\bar{s}}{\partial t^2}\,\frac{R^2}{B}\,I_{1_{ij}}}} + \underline{\underline{\frac{\partial\bar{c}}{\partial t}\,\frac{\rho}{\bar{r}}\,\frac{PR}{B}\,I_{1_{ij}}}} = \left\{-\frac{1}{B}\,([\bar{k}_y + \bar{k}_{ds}] + \underline{\underline{B_s}})\bar{s} + \frac{\rho}{\bar{r}}\,\frac{1}{B}\,([\bar{k}_c + \bar{\alpha}_c\eta_0] + \underline{\underline{B_c}})\bar{c} - \underline{\underline{\frac{\partial\bar{c}}{\partial x_1}\,\frac{\rho}{\bar{r}}\,\frac{\bar{v}}{\gamma}\,\frac{P}{B}\,I_{1_{ij}}}}\right\} \tag{30b}$$

where new terms appearing in the mean equations that differ from the local equations (1a) and (1b) are understruck, γ is $\bar{v}n/K_gJ_1$, $I_{1_{ij}}$ is $(\sigma_f^2\lambda_1/\bar{v})(1 - \exp[-\bar{v}t/\lambda_1(\chi + 1)])/(\chi +$

1), $I_{4_{ij}}^{(m)}$ $(m = 1, \ldots, 5)$ is $(\sigma_{\delta m}^2 \lambda_{1m}/\bar{v})(1 - \exp[-\bar{v}t/\lambda_{1m}(\chi + 1)])/(\chi + 1)$, χ is $-(\lambda_1/\bar{v})(A_c + (B_s/B))$, v_e is $[\bar{v} - 2I_{1_{ij}}(\bar{v}/\gamma)(P + b_4)]$, and

$$A_c = [\sigma_f^2(b_3\eta_1 + \bar{\alpha}_c\eta_3 + \bar{v}/\gamma(b_3\eta_2 + \bar{\alpha}_c\eta_4)) - I_{1_{ij}}((P + b_4)^2 + PQ) - (I_{4_{ij}}^{(1)} + \eta_0^2 I_{4_{ij}}^{(3)} + I_{4_{ij}}^{(4)})]$$

$$B_c = \left[\sigma_f^2(b_3\eta_1 + \bar{\alpha}_c\eta_3 + \bar{v}/\gamma(b_3\eta_2 + \bar{\alpha}_c\eta_4)) - (I_{4_{ij}}^{(1)} + \eta_0^2 I_{4_{ij}}^{(3)}) - I_{1_{ij}}P((P + b_4) + Q + (\bar{k}_{ds}R + b_5)) - \frac{\partial I_{1_{ij}}}{\partial t} PR \right]$$

$$A_x = [\sigma_f^2 R b_2 - I_{1_{ij}}Q((P + b_4) + Q + (\bar{k}_{ds}R + b_5)) - I_{4_{ij}}^{(2)}]$$

$$B_s = \left[\sigma_f^2 R(b_2 + b_5) - I_{1_{ij}}(PQ + [Q + (\bar{k}_{ds}R + b_5)]^2) - \frac{\partial I_{1_{ij}}}{\partial t} R(Q + (\bar{k}_{ds}R + b_5)) - (I_{4_{ij}}^{(2)} + I_{4_{ij}}^{(5)}) \right]$$

$$B = 1 - 2R(Q + \bar{k}_{ds}R) - R^2 \frac{\partial I_{1_{ij}}}{\partial t}$$

(detachment and inactivation of attached viruses)

$$P = b_1 + \bar{\alpha}_c\eta_1 + b_3\eta_0 + \bar{\alpha}_c\eta_2\bar{v}/\gamma$$

(attachment of free viruses)

$$Q = \bar{k}_y R + b_2 \qquad \text{(detachment of attached viruses)}$$

$$R = \frac{\rho_s a_r b_r K_g^{b_r}}{\bar{r}}$$

On the basis of a comparison of the form of the mean equations (16) above with the system of equations solved as an intermediate step (appendix A), the unknown coefficients introduced in the intermediate time transformation step are found to be $\alpha_1 = -[(\bar{k}_{dc} + \bar{k}_c + \bar{\alpha}_c\eta_0) + A_c]$ and $\beta_2 = -(1/B)[(\bar{k}_y + \bar{k}_{ds}) + B_s]$, respectively.

Equations (30a) and (30b) illustrate that the incorporation of spatial heterogeneity gives rise to a transport equation that differs significantly in form from that of the local model. We quantify this significance later in this paper. Original coefficients (multiplying gradients and concentrations) have been modified considerably, and several new terms appear that were not present in the original local-scale equations. The free virus effective velocity is now a function of aquifer heterogeneity parameters as well as virus transport parameters (filtration, adsorption, and inactivation). Similarly, longitudinal dispersion is a function of aquifer and virus transport parameters, and coefficients multiplying free and attached virus concentrations contain additional terms. Of particular interest, products of attachment terms and detachment terms appear several times, an effect which could not have been predicted a priori. Time derivatives for both free and attached viruses appear in both conservation equations, and new spatial gradient terms are now present. Results initially appear counterintuitive: "Loss" of free viruses in (30a) now depends on detachment as well as on the spatial variability of filtration and adsorption. "Gain" of detaching viruses in (30a) is a function of attachment parameters. It is a formidable if not impossible task to visually inspect (30a) and (30b) to quantitatively interpret the effects of incorporating heterogeneity on virus transport.

Table 2. Base-Case Input Parameters for Mean Simulations

Variable	Definition	Value
K_g	mean hydraulic conductivity, exp $(\bar{f})$	112 m d^{-1}
σ_f^2	ln K variance	0.24
λ_1	horizontal correlation scale	3.6 m
J_1	mean hydraulic gradient	0.0015
$\bar{v}$	mean pore water velocity	0.42 m d^{-1}
α_L	local longitudinal dispersivity	0.01 m
d_p	mean virus diameter	0.1 μm
η_0	single collector efficiency parameter	660 d^{-1}
$\bar{k}_c$	mean adsorption coefficient	0.0
a_1	first adsorption coefficient	0.0
b_1	second adsorption coefficient	0.0
CV$_1$	coefficient of variation of δ_1	0.0
$\bar{k}_y$	mean detachment rate	0.09 d^{-1}
a_2	first detachment coefficient	0.09 d^{-1}
b_2	second detachment coefficient	0.0
CV$_2$	coefficient of variation of δ_2	0.5
$\bar{\alpha}_c$	mean collision efficiency	0.007
a_3	first collision efficiency coefficient	0.0001
b_3	second collision efficiency coefficient	0.00104
CV$_3$	coefficient of variation of δ_3	0.5
$\bar{k}_{dc}$	free virus inactivation rate	0.0
$\bar{k}_{ds}$	attached virus inactivation rate	0.0

3. Stochastic Mean Simulations

In order to determine whether the new terms in the mean equations specified by (30) represent significant effects on the virus transport process, numerical simulations implementing (30) were conducted to quantify the effects of heterogeneity on mean one-dimensional virus transport. Simulated conditions represent, for example, the transport of viruses from the center of a constant source trench (or line of wells) into a steady flow field or virus transport along an individual groundwater flow line (e.g., the experimental setup used by *Schijven et al*. [1997]). Finite differences (fully implicit Euler scheme) were used to represent the system of mean equations, and simulations were run for a period of 2 years over a scale of 750 m. Spatial and temporal discretizations were selected based on grid Peclet number (less than or equal to 10) and Courant number (less than 1) criteria to be 0.1 m and 1 hour, respectively, for the majority of the simulations. The details of the finite difference scheme and the FORTRAN code developed to implement the scheme are provided by *Rehmann* [1998].

Aquifer characteristics (σ_f^2, λ_1, K_g, J_1, $\bar{v}$, and α_L) for the Cape Cod, Massachusetts, study site are used as a base case and are summarized in Table 2 along with other base-case parameters. For illustrative purposes, breakthrough curves 36 m from the source are shown below for a number of different scenarios. This distance was chosen because it is 10 times the horizontal correlation scale (3.6 m) of the aquifer [*Hess et al*., 1992] thereby allowing the viruses or colloids sufficient travel distance to justify the ergodicity assumption. The mean collision efficiency value ($\bar{\alpha}_c = 0.007$) is based on field studies conducted at Cape Cod by *Harvey and Garabedian* [1991], and the mean detachment rate (0.09 d^{-1}) is based on typical values observed in laboratory and field studies [e.g., *Kinoshita et al*., 1993; *Bales et al*., 1991]. Correlation coefficients for collision efficiency (a_3 and b_3) were obtained by selecting a second practical data value, based on observations that attachment increases with decreasing hydraulic conductivity [e.g., *Morley et al*., 1998] and fitting a line to the two data points. In the base-case model, detachment was not correlated to hydraulic conductivity (again in order to focus on filtration effects).

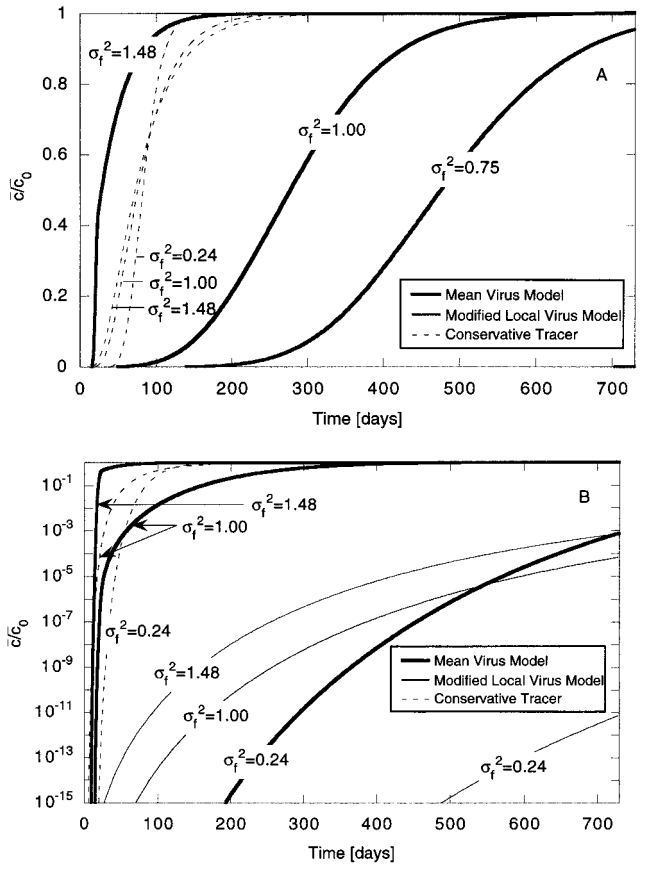

Figure 2. Sensitivity of breakthrough to σ_f^2 (a) on linear scale and (b) on logarithmic scale. Breakthrough curves of mean virus transport (solid bold curves), modified local virus transport (solid thin curves), and a conservative tracer (dashed curves) for the base-case parameters, indicated in Table 2, with sensitivity to σ_f^2 are shown.

Stochastic or mean breakthrough curves are compared to those of a conservative tracer and those of the local virus transport model. In this paper the "local" model of virus transport as applied to the field is implemented by using (1a) and (1b) but with constant macrodispersion added to local dispersion, which is typically the way that the local-scale virus transport model has been used in previous larger-scale transport studies [see, e.g., *Yates*, 1995]. This allows relevant comparison of the "scaled up" local model to the stochastic mean virus transport model and to a field-scale model of a conservative chemical tracer. If this adjustment were not made, the comparison of the local-scale virus transport model to the stochastic mean model would be unclear because of the disparity in local versus macrodispersivity values. This "scaled up" local model will be referred to henceforth as the modified local model. Similarly, macrodispersion was incorporated into the conservative tracer simulations.

3.1. Sensitivity to Aquifer Parameters

Figure 2 shows the effect of varying σ_f^2 while holding all other parameters constant. The modified local model breakthrough curves differ significantly from those of the stochastic model, with stochastic model breakthrough occurring much earlier than modified local model breakthrough. Modified local breakthrough curves for even the highest ln K variance value (1.48) do not even appear on the linear scale plot shown. For a fairly heterogeneous aquifer, characterized by an ln K variance of 1.48, the mean model free virus concentration has leveled off to about the inflow value starting at approximately 160 days. Conversely, the modified local model shows a concentration of only 0.1% of the influent concentration after 2 years, illustrating the significant impact of the added effects of spatial variability on virus transport.

Another significant effect shown in Figure 2 is that of increasing ln K variance on the stochastic model output. As σ_f^2 increases, virus breakthrough occurs sooner. When a very high σ_f^2 is used, virus breakthrough can actually precede that of a conservative tracer. Early breakthrough of microorganisms compared to that of a conservative tracer has been observed in several studies [e.g., *Powelson et al*., 1993; *Toran and Palumbo*, 1992; *Bales et al*., 1989] and has been attributed to virus transport in preferential flow paths or size exclusion effects. A high ln K variance implies that more of the aquifer is characterized by the tails of the ln K distribution. The "high ln K" tail may be thought of as very conductive lenses through which viruses are directed thus leading to faster virus transport. The increased aquifer volume included in the "low ln K" tail would also contribute to the size exclusion effect, as less of the aquifer would be accessible to viruses. Extremely high σ_f^2 values (e.g., 4.0) caused model aberrations, most likely reflecting the limitations of the small perturbation approach.

Figure 3 shows the effect of increasing the mean ln K value (K_g) on virus transport. In order to maintain the same mean pore velocity for the different K_g values, the hydraulic gradient value (J_1) was adjusted. Breakthrough curves are shown for four mean ln K values: 112, 750, 4200, and 2.5×10^4 m d^{-1}, corresponding to a range of soils from clean sand to coarse gravel. Variations in mean ln K values affect mean transport parameters, in this case $\bar{\alpha}_c$, where attachment efficiency decreases for more conductive materials. This effect was observed by *Morley et al*. [1998] and has been attributed to such factors as the high relative abundance of iron-rich mineral deposits in finer-grained materials, leading to increased attachment efficiency [*Harvey et al*., 1993]. In addition, recent work by H. Dong (personal communication, 1999) has also shown a negative correlation between collision efficiency and grain size for a series of soil columns.

Figure 3 illustrates that the stochastic and modified local models differ the most for the lower K_g values selected, with the stochastic breakthrough curves greatly preceding the modified local breakthrough curves. For the smallest K_g value used (112 m d^{-1}), the absolute concentration values are so small that, even though the curves differ by approximately 8 orders of magnitude, these effects cannot be seen on the linear plot in Figure 3. As K_g increases, the modified local and stochastic models approach each other. For K_g equal to 4200 m d^{-1}, the modified local and stochastic models differ slightly, and in the highest K_g case (2.5×10^4 m d^{-1}) the stochastic and modified local model breakthrough curves coincide, indicating that heterogeneity does not play a significant role in a very conductive aquifer and therefore that the modified local model may be sufficient for modeling virus breakthrough in this case. For the highest K_g value, virus breakthrough approaches tracer breakthrough but does not precede it, suggesting that early virus breakthrough is attributable to heterogeneity and not high mean ln K values.

In addition, as the mean ln K value is increased, the effect of aquifer heterogeneity on virus breakthrough decreases. The

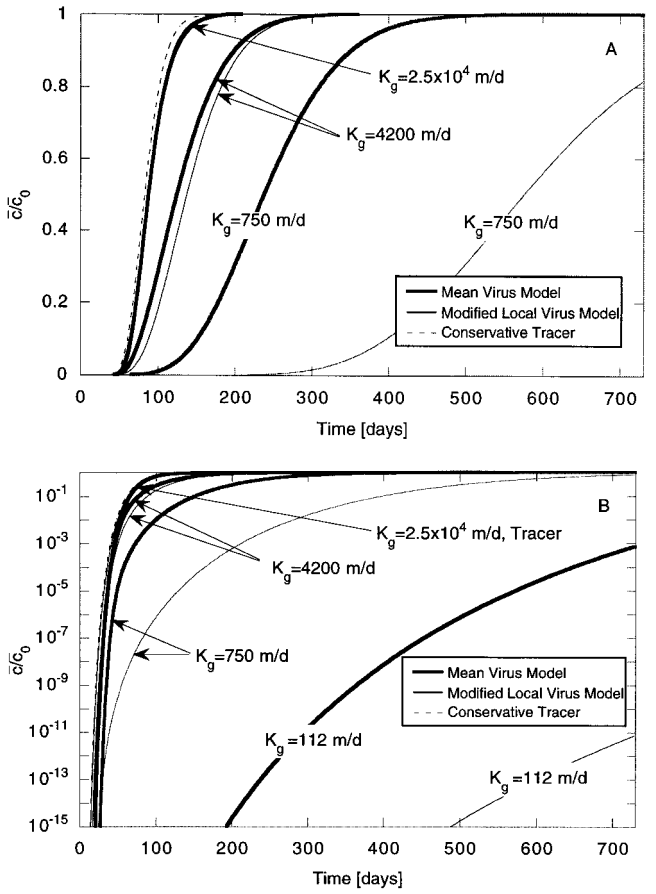

Figure 3. Sensitivity of breakthrough to K_g (a) on linear scale and (b) on logarithmic scale. Breakthrough curves of mean virus transport (solid bold curves), modified local virus transport (solid thin curves), and a conservative tracer (dashed curves) for the base-case parameters indicated in Table 2, with sensitivity to K_g are shown.

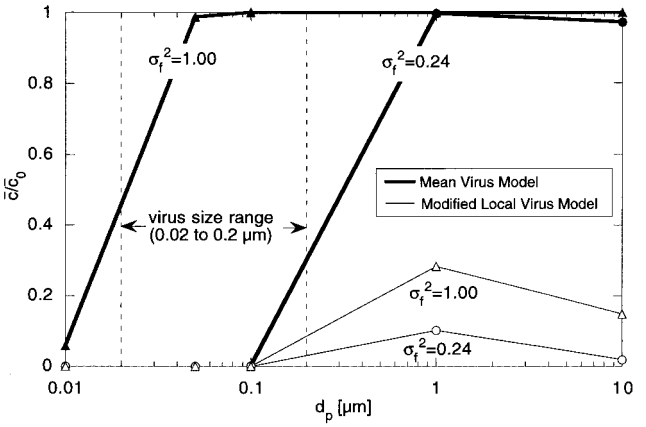

Figure 4. Sensitivity analysis of d_p for different ln K variance values. Colloid diameter d_p versus scaled mean free virus concentration (solid bold curves) and modified local free virus concentration (solid thin curves) for the base-case parameters indicated in Table 2 with sensitivity to ln K variance are shown. Normalized concentrations are at $x = 36$ m after 2 years. The larger particle sizes (1–10 μm) represent size classes that are considerably larger than the viruses for which the model was developed. Consequently, predictive capability of the model may be less accurate for the larger particles because the effect of gravity does not appear to be adequately captured.

stochastic model essentially predicts a higher dependence on σ_f^2 for a less conductive aquifer than for a more conductive aquifer. The mean simulation results also suggest that as the aquifer becomes increasingly conductive, filtration would play a smaller role in transport, which intuitively makes sense. As an extreme case, a colloid of 0.1 μm diameter injected into a gravel and cobble aquifer would be expected to behave like a conservative tracer, as interactions with solid surfaces would be minimal. Consequently, spatial variability of aquifer parameters may not be very important, and the stochastic and modified local model output would be very similar. At the other end of the scale a virus injected into a tight sand and silt formation would have extensive surface interactions. Heterogeneity in transport parameters in this case would play a much larger role, leading to significantly different modified local and stochastic model results. Because transport parameters are coupled to ln K in this model, higher ln K variability implies, to some degree, higher transport parameter variability.

Varying a third aquifer parameter, horizontal correlation scale (λ_1), had a minimal effect on virus transport, and therefore the simulation results testing this sensitivity are not shown. Virus breakthrough occurs earlier for larger correlation scales; increasing λ_1 from 1.0 to 3.5 m has more of an effect than an increase from 5.0 to 10.0 m, indicating that an asymptotic effect may be occurring. Increasing the horizontal correlation scale reflects an increased persistence in the horizontal soil lenses, which could lead to viruses traveling farther in high-conductivity lenses without encountering low-conductivity materials. Despite this persistence in horizontal soil lenses, virus breakthrough is much later than tracer breakthrough for all values of λ_1 tested. Because the horizontal correlation scale does not vary over several orders of magnitude (unlike K_g and σ_f^2), one would not expect as significant differences in breakthrough curves in this sensitivity analysis.

3.2. Sensitivity to Virus Properties

The basic colloid filtration theory predicts that colloids of diameters approaching 1 μm will be retained the least in a given porous medium because of a combination of factors: Brownian motion (the governing process for very small colloids) is decreasing as the colloid diameter is increasing, and gravity, interception, and London/van der Waal's forces are only beginning to become significant for this particle diameter. Figure 4 shows the effect of varying colloid diameter (d_p) and ln K variance (σ_f^2) on free colloid concentrations at 36 m after 2 years. For both σ_f^2 values of 0.24 and 1.00 the modified local model predicts a maximum concentration for colloid diameters around 1 μm, with the higher ln K variance value yielding slightly higher colloid concentrations. For the stochastic model with σ_f^2 equal to 0.24, maximum concentration is again for a colloid diameter of approximately 1 μm, but the range of colloid diameters for which significant breakthrough has occurred by 2 years is significantly different from the modified local model. Where the modified local model predicts $\bar{c}/\bar{c}_0$ of less than 10^{-10} for a colloid diameter of 0.1 μm, the stochastic model predicts $\bar{c}/\bar{c}_0$ approaching 0.001. When σ_f^2 is increased to 1.0, the lower limit of colloid diameter which is transported the most is decreased even further, so that even colloids as small as 0.01 μm reach a normalized concentration of 0.08 by 2 years.

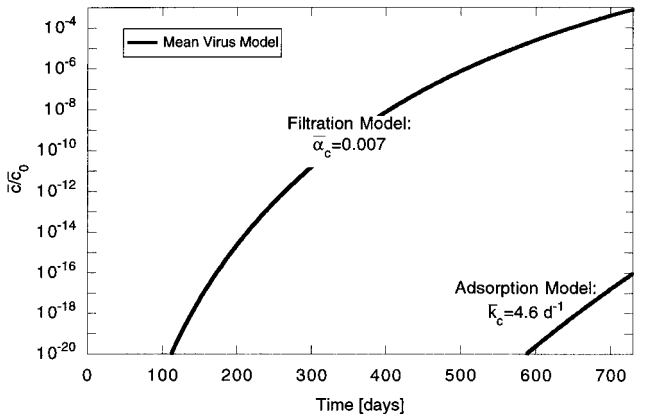

Figure 5. Comparison of breakthrough for filtration-only and adsorption-only models. Breakthrough curves of mean virus transport for the base-case parameters indicated in Table 2, with both adsorption-only and filtration-only models having the same mean "attachment" rates of 4.6 d^{-1} (i.e., $\bar{\alpha}_c \eta_0 = \bar{k}_c = 4.6\ d^{-1}$) are shown.

For the most heterogeneous aquifer the stochastic model predicts that significant breakthrough occurs for colloids throughout the size range of 0.01–10 μm. As the degree of aquifer heterogeneity (i.e., σ_f^2) decreases, only colloids with diameters between 0.1 and 10 μm significantly break through after 2 years. Therefore increasing heterogeneity (σ_f^2) in the stochastic model results in faster breakthrough of the smallest colloids (a size class which includes viruses 0.02–0.2 μm in diameter). Increasing σ_f^2 in the modified local model results in increased macrodispersion and faster breakthrough, but the difference is not as marked as in the case of the stochastic mean virus model. Therefore, in a very heterogeneous aquifer we would expect that colloids of all sizes would be significantly transported. As discussed above, a very heterogeneous aquifer is characterized by regions of very high and very low conductivity. Colloids may be transported easily in the high-conductivity regions regardless of size. As the aquifer heterogeneity decreases, the available high-conductivity lenses also decrease, resulting in colloid transport that is more sensitive to the less conductive materials.

Harvey and Garabedian [1991], in field observations of bacteria being advected down gradient within a plume of organically contaminated groundwater at the Cape Cod U.S. Geological Survey study site, observed that the colloid filtration theory of *Yao et al*. [1971] underpredicted the relative abundance of small bacteria (0.2 μm) and overestimated the relative abundance of the larger bacteria (1.2 and 1.4 μm in particular) 680 m down gradient from the source. On the basis of these observations the stochastic model may account for the increase in the smaller size class but may also overpredict the transport of larger colloids. This may be attributed to gravitational effects that are not captured well by the η^* parameterization. It should be noted that these larger sizes are well above the range of viruses, the latter of which are the focus of this work.

Figure 5 shows a comparison of filtration-only and adsorption-only abiotic virus transport models in which the effective "attachment" rates (4.6 d^{-1}) and detachment rates (0.09 d^{-1}) are equal in both the filtration-only and the adsorption-only cases, and all other parameters are identical in the two models. The filtration-only model predicts significantly earlier breakthrough than the adsorption-only model. In order to force the two breakthrough curves to coincide, either the mean adsorption rate must be significantly decreased or the mean collision efficiency must be increased. Early virus breakthrough for a given hydraulic conductivity field could be modeled using either a moderate mean collision efficiency value in a filtration-only model or a very low mean adsorption rate in an adsorption-only model. Therefore the selected governing process for virus attachment (either adsorption or filtration) significantly affects the interpretation of the virus breakthrough curve.

Because both attachment mechanisms are first-order kinetic functions of the free-virus concentration, it would be possible to generate identical breakthrough curves using either expression. In order to decide which expression best represents virus transport behavior in the field, one approach would be to determine η_0 based on aquifer parameters, fit the first-order rate coefficient (equivalent to $\bar{\alpha}_c \eta_0$ or $\bar{k}_c$) to the data, and back out the mean collision efficiency ($\bar{\alpha}_c$). Depending on the magnitude of $\bar{\alpha}_c$ (i.e., theoretically $0 \leq \bar{\alpha}_c \leq 1$, typically of the order of 0.01), use of the filtration model could be deemed appropriate or inappropriate. It should be noted that the early U.S. EPA-sponsored model VIRALT [*Park et al*., 1991] which simulates virus transport subject to first-order adsorption was found to significantly underpredict virus transport at several field sites [*Yates*, 1995]. If the same first-order attachment rate had been used but with virus filtration as the modeled process, the stochastic results suggest that much more extensive transport would have been predicted (i.e., increased virus concentrations at a particular point in space), better representing observed concentrations.

It is also important to note that the derived mean model is extremely sensitive to the mean collision efficiency value ($\bar{\alpha}_c$). Increasing $\bar{\alpha}_c$ from 0.007 to 0.01 had a significant effect on virus transport predictions, as did increasing the uncorrelated random portion of $\bar{\alpha}_c(\delta_3)$. On the basis of these observations, characterization of $\bar{\alpha}_c$ in the field appears to be an important consideration in accurately modeling field-scale virus transport using the colloid filtration model.

Up to this point, inactivation or first-order decay has been neglected in order to focus discussions on attachment and detachment variability. In this section the effects of varying the inactivation rates of free and attached viruses are investigated. Inactivation is assumed to be uncorrelated to $\ln K$ ($b_4 = b_5 = 0$), and random variability in inactivation is assumed to be zero for the simulations shown in Figure 6. The most complete breakthrough occurs for $\bar{k}_{dc} = \bar{k}_{ds} = 0.0$, since no viruses are being lost to inactivation. If only unattached viruses inactivate, normalized breakthrough concentrations decrease by approximately 2 orders of magnitude from the conservative (no inactivation) case, but concentrations continue to increase after 2 years. If, however, only attached viruses are inactivating, normalized breakthrough concentrations decrease by approximately 16 orders of magnitude and level off after about 300 days. Incorporating both free and attached inactivation results in a further decrease in concentrations of approximately 2 orders of magnitude. On the basis of these results the mean model is more sensitive to attached virus inactivation than it is to free virus inactivation. Similar behavior is seen with the modified local model, but concentrations are several orders of magnitude lower. Therefore, in both the mean and modified local models the incorporation of differing inactivation rates for free and attached viruses has a significant effect on model

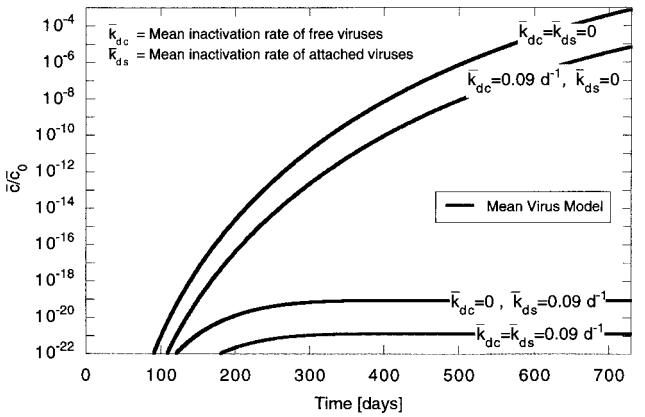

Figure 6. Sensitivity of mean model free virus breakthrough to free ($\bar{k}_{dc}$) and attached ($\bar{k}_{ds}$) virus inactivation rates. Breakthrough curves of mean virus transport for the base-case parameters indicated in Table 2 but including inactivation $\neq 0$ are shown.

predictions. This is an important feature to incorporate because researchers have observed that attached-virus inactivation can occur either more slowly [*Bagdasar'yan*, 1964; *Hurst et al*., 1980; *Sobsey et al*., 1986] or more quickly [*Blanc and Nasser*, 1996] than free-virus inactivation. The stochastic model presented offers insight into the importance of adequately quantifying inactivation, as well as other virus transport and aquifer parameters in modeling and understanding large-scale virus transport in heterogeneous aquifers.

4. Summary and Conclusions

The results of this research indicate that the incorporation of heterogeneity has a marked effect on virus and colloid transport predictions. The spectral stochastic approach was used successfully to incorporate spatial variability into free virus transport and attached virus conservation equations. By taking into consideration heterogeneity of both aquifer and virus transport parameters, a mean conservation model was developed that differs significantly from the local-scale model on which it was based. The resulting mean model equations contain terms that are not present in the local-scale equations, including new temporal and spatial derivatives and additional large-scale attachment, detachment, and inactivation terms. These macroscopic coefficients are not easily separated into the categories of attachment, detachment, and inactivation because they include products and quotients of these input parameters.

In order to observe the overall effect of heterogeneity on virus transport, mean numerical simulations were conducted. A finite difference code was developed to simulate one-dimensional, mean virus transport under steady flow conditions. Breakthrough curves incorporating all effects simultaneously led to a more complete understanding of large-scale transport. Major results from these mean numerical simulations are summarized as follows:

1. Incorporation of spatial variability resulted in faster virus transport, implying earlier breakthrough and higher peak concentrations. These results showed that local models applied at the field scale may significantly underestimate virus transport in heterogeneous aquifers, as has been observed in other work [e.g., *Yates*, 1995].

2. As the porous media becomes increasingly heterogeneous (i.e., as σ_f^2 increases), it was observed that virus transport can be facilitated to such a degree that virus arrival actually preceded the arrival of a conservative tracer. Increased σ_f^2 implied an increasing amount of porous media belonging to the high and low tails of the ln K distribution, reflecting the presence of more high- and low-conductivity lenses. The interpretation of this result is that viruses are excluded from the lowest-conductivity regions because of restrictive pore sizes in fine-grained materials relative to the colloid diameter (e.g., viruses are excluded from certain clays and from internal (intragrain) porosity) but are able to move through the higher conductivity lenses which are characterized by higher pore water velocities. Therefore increasing the degree of heterogeneity resulted in faster breakthrough of viruses transported through the media at the high end of the ln K distribution.

3. As the mean ln K value increased, viruses broke through earlier. Higher-conductivity material is typically characterized by larger soil grains and pore diameters thereby an increased "accessible pore zone" for virus transport. Stochastic mean and modified local breakthrough curves differed the most for less conductive materials, indicating that input parameters play a less significant role in highly conductive aquifers. Because more conductive aquifers would be characterized by fewer virus/grain interactions, it would be anticipated that transport behavior in such aquifers would be closer to that of a conservative tracer (as seen in the mean simulations).

4. The stochastic and modified local models differed greatly in their sensitivity to the virus diameter (d_p). Incorporation of aquifer heterogeneity led to a much greater range of virus diameters for which significant breakthrough occurred. As σ_f^2 increased, breakthrough of the smallest colloids was faster, which could be interpreted as being due to increased availability of accessible pores. In addition, mean model output became less sensitive to σ_f^2 as the mean hydraulic conductivity increased for all diameters tested, although smaller colloids were more sensitive to the aquifer parameters (K_g and σ_f^2) than larger particles. However, the stochastic model may predict a concentration that is too high for the largest colloid sizes (i.e., 1–10 μm, which is greater than the size of viruses which are the focus of this work) because of the poor η^* parameterization of gravity effects.

5. When virus attachment is modeled as first-order adsorption rather than colloid filtration but with the same "attachment" rate (i.e., $\bar{\alpha}_c\eta_0 = \bar{k}_c$), the colloid filtration model predicted significantly earlier breakthrough than the adsorption model. Therefore the more physically based colloid filtration model may capture significant effects in a heterogeneous aquifer which are not incorporated in an empirical adsorption model. Quantification of the mean and variability of the collision efficiency ($\bar{\alpha}_c$) also seems to be an important factor in correctly predicting virus transport in heterogeneous aquifers.

6. As anticipated for the case in which viruses are undergoing first-order inactivation, virus breakthrough was significantly lower than for the "conservative" (nondecaying) case. Inactivation of viruses associated with solid surfaces had a greater effect on breakthrough than inactivation of free viruses, indicating that accounting for differences in inactivation rates between the two phases is an important feature of the stochastic result.

On the basis of a qualitative comparison of numerical results and field observations, the stochastic approach has yielded insight into field-scale transport behavior. For example, early

virus breakthrough attributed to flow through macropores or to size exclusion effects was captured in the stochastic mean model using a higher ln K variance value. In order to predict large-scale virus transport using this approach, some information regarding the degree of aquifer heterogeneity (e.g., σ_f^2 and K_g) would therefore be required. The model output for even the simple conditions of a steady flow field indicate the importance of aquifer and collision efficiency variability on transport.

Tremendous progress has been made in recent years in understanding local-scale virus transport processes and in performing small in situ field-scale studies (i.e., of the order of 10 m). The fundamental results in this paper present one method for incorporating physical heterogeneity into mathematical predictions of virus transport at the larger field scale. In order to further advance our understanding of larger-scale transport and, in turn, develop more physically based wellhead protection programs, quantification of variability of the different input parameters to this model is essential. In future field studies, measurements of the spatial variability of the collision efficiency in particular would be extremely useful in predicting virus transport. In order to comprehensively test the stochastic model, two efforts are needed. First, the model results should be compared to numerical validating experiments to assess the limitations of the theory. Second, if the theory is found to be robust even under a limited set of conditions, then the stochastic model should be compared to an appropriate three-dimensional data set of large-scale virus (or abiotic colloid) transport at a well-characterized field site. To date, no such data set is available. Until it is, the mean virus transport model developed in this paper provides insight into the predicted relationship among local transport processes (advection, dispersion, attachment, detachment, and inactivation) at larger scales, indicating the significant differences between field-scale virus transport evaluated using a laboratory-scale model and a stochastic mean model, and providing a theoretical basis for data collection in the future.

Appendix A

In order to solve this system of equations for $dZ_c(\mathbf{k})$ and $dZ_s(\mathbf{k})$, it is necessary to carry out an intermediate transformation [*Miralles-Wilhelm and Gelhar*, 1996a, b; *Rehmann*, 1998] consisting of three main steps:

1. Solve a simplified system of equations equivalent to (19a) and (19b) in order to obtain $dZ_c(\mathbf{k})$ and $dZ_s(\mathbf{k})$ as functions of the conservative quantities $dZ_{\hat{c}}(\mathbf{k})$ and $dZ_{\hat{s}}(\mathbf{k})$. The equivalent homogeneous set of equations is

$$\frac{\partial dZ_c}{\partial t} = \alpha_1 dZ_c + \beta_1 dZ_s \tag{A1}$$

$$\frac{\partial dZ_s}{\partial t} = \alpha_2 dZ_c + \beta_2 dZ_s \tag{A2}$$

where α_1, α_2, β_1, and β_2 are unknown effective loss and gain coefficients which may differ from the mean values $(-(\bar{k}_{dc} + \bar{k}_c + \bar{\alpha}_c\eta_0)$, $\rho(\bar{k}_c + \bar{\alpha}_c\eta_0)$, $\bar{k}_y\bar{r}/\rho$, and $-\bar{r}(\bar{k}_{ds} + \bar{k}_y)$, respectively). Solution of this system of equations introduces the variables $dZ_{\hat{c}}(\mathbf{k})$ and $dZ_{\hat{s}}(\mathbf{k})$ (which represent conservative perturbation expressions) using the initial condition $dZ_c(\mathbf{k}) = dZ_{\hat{c}}(\mathbf{k})$ and $dZ_s(\mathbf{k}) = dZ_{\hat{s}}(\mathbf{k})$ at time = 0. The result is

$$dZ_c = \left\{ dZ_{\hat{c}} \cdot \frac{[(\alpha_1 - \beta_2)(e^{w_1 t} - e^{w_2 t}) + (e^{w_1 t} + e^{w_2 t})\sqrt{(\alpha_1 - \beta_2)^2 + 4\alpha_2\beta_1}]}{2\sqrt{(\alpha_1 - \beta_2)^2 + 4\alpha_2\beta_1}} + dZ_{\hat{s}} \frac{\beta_1(e^{w_1 t} - e^{w_2 t})}{\sqrt{(\alpha_1 - \beta_2)^2 + 4\alpha_2\beta_1}} \right\} \tag{A4}$$

$$dZ_s = \left\{ dZ_{\hat{s}} \cdot \frac{[-(\alpha_1 - \beta_2)(e^{w_1 t} - e^{w_2 t}) + (e^{w_1 t} + e^{w_2 t})\sqrt{(\alpha_1 - \beta_2)^2 + 4\alpha_2\beta_1}]}{2\sqrt{(\alpha_1 - \beta_2)^2 + 4\alpha_2\beta_1}} + dZ_{\hat{c}} \frac{\alpha_2(e^{w_1 t} - e^{w_2 t})}{\sqrt{(\alpha_1 - \beta_2)^2 + 4\alpha_2\beta_1}} \right\} \tag{A4}$$

where

$$w_1 = \tfrac{1}{2}[(\alpha_1 + \beta_2) + \sqrt{(\alpha_1 - \beta_2)^2 + 4\alpha_2\beta_1}]$$

$$w_2 = \tfrac{1}{2}[(\alpha_1 + \beta_2) - \sqrt{(\alpha_1 - \beta_2)^2 + 4\alpha_2\beta_1}]$$

2. Substitute these simplified solutions for $dZ_c(\mathbf{k})$ and $dZ_s(\mathbf{k})$ in terms of $dZ_{\hat{c}}(\mathbf{k})$ and $dZ_{\hat{s}}(\mathbf{k})$ back into the original system of equations (19a) and (19b) to obtain a coupled system of ordinary differential equations for the conservative quantities $dZ_{\hat{c}}(\mathbf{k})$ and $dZ_{\hat{s}}(\mathbf{k})$. This coupled system of equations is solved for these variables to yield two independent solutions:

$$dZ_{\hat{c}} = F_1(t)\,\frac{1 - e^{-\beta^* t}}{\beta^*} \tag{A5}$$

$$dZ_{\hat{s}} = F_2(t)\,\frac{1 - e^{-\beta^* t}}{\beta^*} \tag{A6}$$

where

$$\beta^* = [ik_1\bar{v} + k_i k_j D_{ij} + ((\bar{k}_c + \bar{\alpha}_c\eta_0 + \bar{k}_{dc}) + \alpha_1)] + [(\bar{k}_y + \bar{k}_{ds}) + \beta_2]$$

$$F_1(t) = (f_1 - a_1 f_2)/(1 - a_1 a_2)$$

$$F_2(t) = (f_2 - a_2 f_1)/(1 - a_1 a_2)$$

$$a_1 = 2\beta_1 E_1/[E_1(\alpha_1 - \beta_2) + E_2\sqrt{G}]$$

$$a_2 = 2\alpha_2 E_1/[-E_1(\alpha_1 - \beta_2) + E_2\sqrt{G}]$$

$$G = (\alpha_1 - \beta_2)^2 + 4\alpha_2\beta_1$$

$$E_1 = e^{w_1 t} - e^{w_2 t}$$

$$E_2 = e^{w_1 t} + e^{w_2 t}$$

$$f_1 = \frac{2\sqrt{G}}{[E_1(\alpha_1 - \beta_2) + E_2\sqrt{G}]} \cdot \left\{ dZ_f \left[-\bar{c}(b_1 + \bar{\alpha}_c\eta_1 + b_3\eta_0) + \frac{\bar{r}}{\rho}\bar{s}\left(\bar{k}_y \frac{1}{\bar{r}}\,\rho_s a_r b_r K_g^{b_r} + b_2 \right) \right] - dZ_{v_i}\left(\bar{c}\,\bar{\alpha}_c\eta_2 + \frac{\partial \bar{c}}{\partial \zeta_i} \right) - \bar{c}(dZ_{\delta_1} + \eta_0 dZ_{\delta_3}) + \frac{\bar{r}}{\rho}\bar{s}\,dZ_{\delta_2} \right\}$$

$$f_2 = \frac{2\sqrt{G}}{(-E_1(\alpha_1 - \beta_2) + E_2\sqrt{G})} \left\{ dZ_f \left[\frac{\rho}{\bar{r}} \bar{c}(b_1 + \bar{\alpha}_c\eta_1 + b_3\eta_0) - \frac{\partial \bar{s}}{\partial t} \frac{1}{\bar{r}} \rho_s a_r b_r K_g^{b_r} - \bar{s}\left(\frac{1}{\bar{r}} \rho_s a_r b_r K_g^{b_r} (\bar{k}_y + \bar{k}_{ds}) + b_2 \right) \right] + \frac{\rho}{\bar{r}} \bar{c}\bar{\alpha}_c\eta_2 dZ_{v_i} + \frac{\rho}{\bar{r}} \bar{c}(dZ_{\delta_1} + \eta_0 dZ_{\delta_3}) - \bar{s} dZ_{\delta_2} \right\}$$

3. Last, obtain uncoupled expressions for the Fourier-Stieltjes amplitudes for both free and attached viruses ($dZ_c(\mathbf{k})$ and $dZ_s(\mathbf{k})$) by substituting (A5) and (A6) back into (A3) and (A4). The uncoupled expressions for $dZ_c(\mathbf{k})$ and $dZ_s(\mathbf{k})$ are

$$dZ_c = \frac{1 - e^{-\beta^* t}}{\beta^*} \left\{ dZ_f \left[-\bar{c}(\bar{\alpha}_c\eta_1 + b_1 + b_3\eta_0 + b_4) + \bar{s}\left(\bar{k}_y \frac{\rho_s a_r b_r K_g^{b_r}}{\rho} + b_2 \frac{\bar{r}}{\rho} \right) \right] + dZ_{v_i}[G_i - \bar{c}\bar{\alpha}_c\eta_2] - dZ_{\delta_1}[\bar{c}] + dZ_{\delta_2}\left[\bar{s}\frac{\bar{r}}{\rho} \right] - dZ_{\delta_3}[\bar{c}\eta_0] \right\} \quad \text{(A7)}$$

$$dZ_s = \frac{1 - e^{-\beta^* t}}{\beta^*} \left\{ dZ_f \left[\bar{c}\frac{\rho}{\bar{r}}(\bar{\alpha}_c\eta_1 + b_1 + b_3\eta_0) - \frac{\partial \bar{s}}{\partial t} \frac{\rho_s a_r b_r K_g^{b_r}}{\bar{r}} - \bar{s}\left((\bar{k}_{ds} + \bar{k}_y) \frac{\rho_s a_r b_r K_g^{b_r}}{\bar{r}} + b_2 \right) \right] + dZ_{v_i}\left[\frac{\rho}{\bar{r}} \bar{c}\bar{\alpha}_c\eta_2 \right] + dZ_{\delta_1}\left[\frac{\rho}{\bar{r}} \bar{c} \right] + dZ_{\delta_3}\left[\frac{\rho}{\bar{r}} \bar{c}\eta_0 \right] - dZ_{\delta_2}[\bar{s}] \right\} \quad \text{(A8)}$$

where $G_i = -\partial \bar{c}/\partial \zeta_i$. These final expressions are used to evaluate the cross-perturbation terms in the mean equations (16a) and (16b).

Appendix B

The integrals in the cross perturbations of (21) through (29) were evaluated for the highly stratified case in which $\delta = \lambda_3/\lambda_1 \ll 1$ ($\lambda_1 = \lambda_2$) [*Gelhar*, 1987]. The cross-perturbation terms expressed in (16a) and (16b) can be defined in terms of four integrals,

$$\overline{f' v_i'} = \frac{\bar{v}}{\gamma} I_{2_{ij}} \quad \text{(B1)}$$

$$\overline{f' c'} = \left[\left(-\bar{c}[\bar{\alpha}_c\eta_1 + b_1 + b_3\eta_0 + b_4] + \bar{s}\frac{\bar{r}}{\rho}\left[\bar{k}_y \frac{\rho_s a_r b_r K_g^{b_r}}{\bar{r}} + b_2 \right] \right) I_{1_{ij}} + (G_j - \bar{c}\bar{\alpha}_c\eta_2) I_{2_{ij}} \right] \quad \text{(B2)}$$

$$\overline{v_i' c'} = \left[\left(-\bar{c}(\bar{\alpha}_c\eta_1 + b_1 + b_3\eta_0 + b_4) + \bar{s}\frac{\bar{r}}{\rho}\left(\bar{k}_y \frac{\rho_s a_r b_r K_g^{b_r}}{\bar{r}} + b_2 \right) \right) I_{2_{ij}} + (G_j - \bar{c}\bar{\alpha}_c\eta_2) I_{3_{ij}} \right] \quad \text{(B3)}$$

$$\overline{f' s'} = \left\{ \left[\bar{c}\frac{\rho}{\bar{r}}(\bar{\alpha}_c\eta_1 + b_1 + b_3\eta_0) - \frac{\partial \bar{s}}{\partial t} \frac{\rho_s a_r b_r K_g^{b_r}}{\bar{r}} - \bar{s}\left((\bar{k}_{ds} + \bar{k}_y) \frac{\rho_s a_r b_r K_g^{b_r}}{\bar{r}} + (b_2 + b_5) \right) \right] I_{1_{ij}} + \frac{\rho}{\bar{r}} \bar{c}\bar{\alpha}_c\eta_2 I_{2_{ij}} \right\} \quad \text{(B4)}$$

$$\overline{c' \delta_1'} = -\bar{c} I_{4_{ij}}^{(1)} \quad \text{(B5)}$$

$$\overline{s' \delta_2'} = -\bar{s} I_{4_{ij}}^{(2)} \quad \text{(B6)}$$

$$\overline{c' \delta_3'} = -\bar{c}\eta_0 I_{4_{ij}}^{(3)} \quad \text{(B7)}$$

$$\overline{c' \delta_4'} = -\bar{c} I_{4_{ij}}^{(4)} \quad \text{(B8)}$$

$$\overline{s' \delta_5'} = -\bar{s} I_{4_{ij}}^{(5)} \quad \text{(B9)}$$

where

$$I_{1_{ij}} = \int_{-\infty}^{\infty} \int \int \left(\frac{1 - e^{-\beta^* t}}{\beta^*} S_{ff}(\mathbf{k})\, d\mathbf{k} \right) \quad \text{(B10)}$$

$$I_{2_{ij}} = \int_{-\infty}^{\infty} \int \int \left(\frac{1 - e^{-\beta^* t}}{\beta^*} S_{fv_j}(\mathbf{k})\, d\mathbf{k} \right) \quad (j = 1, \cdots, 3) \quad \text{(B11)}$$

$$I_{3_{ij}} = \int_{-\infty}^{\infty} \int \int \left(\frac{1 - e^{-\beta^* t}}{\beta^*} S_{v_i v_j}(\mathbf{k})\, d\mathbf{k} \right) \quad (j = 1, \cdots, 3) \quad \text{(B12)}$$

$$I_{4_{ij}}^{(m)} = \int_{-\infty}^{\infty} \int \int \left(\frac{1 - e^{-\beta^* t}}{\beta^*} S_{\delta_m \delta_m}(\mathbf{k})\, d\mathbf{k} \right)$$

$$(m = 1, \cdots, 5 \text{ not a summation index}) \quad \text{(B13)}$$

where integrals are over wave number space (k_1, k_2, and k_3) and $\beta^* = (ik_1\bar{v} + k_i k_j D_{ij} + \beta_0)$, $\beta_0 = [((\bar{k}_c + \bar{\alpha}_c\eta_0 + \bar{k}_{dc}) + \alpha_1) + (\bar{k}_y + \bar{k}_{ds} + \beta_2)]$, and

$$S_{ff}(\mathbf{k}) = \frac{\sigma_f^2 \lambda_1 \lambda_2 \lambda_3}{\pi^2(1 + \lambda_1^2 k_1^2 + \lambda_2^2 k_2^2 + \lambda_3^2 k_3^2)^2} \quad \text{(B14)}$$

$$S_{\delta_i \delta_i}(\mathbf{k}) = \frac{\sigma_{\delta_i}^2 \lambda_{1_i} \lambda_{2_i} \lambda_{3i}}{\pi^2(1 + \lambda_{1_i}^2 k_1^2 + \lambda_{2_i}^2 k_2^2 + \lambda_{3_i}^2 k_3^2)^2} \quad \text{(B15)}$$

In all simulations presented in this paper, it is assumed that the correlation scales for the random portions of the adsorption, collision efficiency, and detachment coefficients are equal to the ln K correlation scales [see, e.g., *Miralles-Wilhelm and Gelhar*, 1996b]. From *Gelhar and Axness* [1983, equation (28a)] the Fourier-Stieltjes amplitude for specific discharge for an anisotropic porous medium is derived in terms of the Fourier-Stieltjes amplitude for hydraulic conductivity. For the case in which the x_1 axis is aligned with the mean flow direction such that $\bar{v}_1 = \bar{v}$, $\bar{v}_2 = \bar{v}_3 = 0$ and for the case of mean flow parallel to the bedding assumed in this paper where $J_2 = J_3 = 0$, the corresponding Fourier-Stieltjes amplitude for mean pore velocity can be inferred to be

$$dZ_{v_j}(\mathbf{k}) = \frac{K_g J_1}{n} \left(\delta_{j1} - \frac{k_j k_1}{k^2} \right) dZ_f(\mathbf{k}) \quad \text{(B16)}$$

where δ_{j1} is the Kronecker delta ($\delta_{j1} = 1$ for $j = 1$ and $= 0$ for $j \neq 1$), $k^2 = k_1^2 + k_2^2 + k_3^2$, and terms are summed over j. Recalling that $S_{fv_j}(\mathbf{k})d\mathbf{k} = E[dZ_f(\mathbf{k})dZ_{v_j}^*(\mathbf{k})]$ and $S_{v_i v_j}(\mathbf{k})d\mathbf{k} = E[dZ_{v_i}(\mathbf{k})dZ_{v_j}^*(\mathbf{k})]$, each integral is evaluated

using the following steps: (1) Multiply through by the complex conjugate of the denominator. (2) Make the change of variables $u_i = \lambda_i k_i$ and neglect local dispersion, since local dispersivity is small relative to the horizontal correlation scale. (3) Express exponentials as a complex sum, that is, $e^{-(iu_1\bar{v}t/\lambda_1)} = \cos(u_1\bar{v}t/\lambda_1) - i\sin(u_1\bar{v}t/\lambda_1)$ thereby allowing elimination of all odd terms in integral variables since these will contribute nothing to the integral. (4) Take $\delta = \lambda_3/\lambda_1 \ll 1 (\lambda_1 = \lambda_2)$. (5) Integrate the components of each expression. Following this methodology, each integral is evaluated analytically and is found to be

$$I_{1_{ij}} = \frac{\sigma_f^2\lambda_1}{\bar{v}} \frac{1 - \exp[-\bar{v}t/\lambda_1(\chi+1)]}{(\chi+1)} \tag{B17}$$

$$I_{2_{ij}} = \frac{\bar{v}}{\gamma} I_{1_{ij}} \tag{B18}$$

$$I_{3_{1j}} = \frac{\bar{v}^2}{\gamma^2} I_{1_{ij}} \tag{B19}$$

$$I_{4_{ij}}^{(m)} = \frac{\sigma_{\delta m}^2\lambda_{1m}}{\bar{v}} \frac{1 - \exp[-\bar{v}t/\lambda_{1m}(\chi+1)]}{(\chi+1)} \tag{B20}$$

where

$$\gamma = \frac{\bar{v}n}{K_g J_1} \quad \text{and} \quad \chi = \frac{\lambda_1}{\bar{v}}\{[(\bar{k}_c + \bar{\alpha}_c\eta_0 + \bar{k}_{dc}) + \alpha_1] + [(\bar{k}_y + \bar{k}_{ds}) + \beta_2]\}.$$

Notation

$A_s = 2[1 - (1-n)^{5/3}]/[2 - 3(1-n)^{1/3} + 3(1-n)^{5/3} - 2(1-n)^2]$.

$A_c = \sigma_f^2(b_3\eta_1 + \bar{\alpha}_c\eta_3 + \bar{v}/\gamma(b_3\eta_2 + \bar{\alpha}_c\eta_4)) - I_{1_{ij}}((P + b_4)^2 + PQ) - (I_{4_{ij}}^{(1)} + \eta_0^2 I_{4_{ij}}^{(3)} + I_{4_{ij}}^{(4)})$.

$A_x = \sigma_f^2 R b_2 - I_{1_{ij}} Q((P + b_4) + Q + (\bar{k}_{ds}R + b_5)) - I_{4_{ij}}^{(2)}$.

$A(v)$ coefficient relating η^* to pore water velocity (e.g., for diffusion $\eta^* = A(v)$ exp $(c_{10} \ln K)$, $A(v) = a_{10} + b_{10}v$), day^{-1}.

$a_{1P} = 6d_p^{-2/3}(3\pi\mu/B_zT)^{-2/3}$.

$a_{1L} = 1.5d_p^{13/8}(4H/9\pi\mu)^{1/8}$.

$a_{1G} = (3/2)(0.00338)d_p^2[(\rho_p - \rho)g/(18\mu)]^{1.2}$.

a_{10}, b_{10}, c_{10} fitting coefficients for the diffusion portion of single collector efficiency.

a_{11}, b_{11}, c_{11} fitting coefficients for the Van der Waal's forces portion of single collector efficiency.

a_{12}, b_{12}, c_{12} fitting coefficients for the gravitational effects portion of single collector efficiency.

a_i, b_i parameters relating virus adsorption ($i = 1$), virus detachment ($i = 2$), collision efficiency ($i = 3$), inactivation of free viruses ($i = 4$), and inactivation of attached viruses ($i = 5$) to ln K (e.g., $k_c = a_1 + b_1 \ln K + \delta_1$).

a_r, b_r fitting constants relating $r(=\rho_b/n)$ to ln K.

α_c collision efficiency factor.

$\bar{\alpha}_c$ mean collision efficiency factor.

α_c' perturbation in collision efficiency.

α_L local longitudinal dispersivity, m.

α_T local transverse dispersivity, m.

α_1 effective loss coefficient for free viruses, day^{-1}.

α_2 effective gain coefficient for attached viruses, day^{-1}.

$B = 1 - 2R(Q + \bar{k}_{ds}R) - R^2(\partial I_{1_{ij}}/\partial t)$.

$B_c = [\sigma_f^2(b_3\eta_1 + \bar{\alpha}_c\eta_3 + \bar{v}/\gamma(b_3\eta_2 + \bar{\alpha}_c\eta_4)) - (I_{4_{ij}}^{(1)} + \eta_0^2 I_{4_{ij}}^{(3)}) - I_{1_{ij}}P((P + b_4) + Q + (\bar{k}_{ds}R + b_5)) - (\partial I_{1_{ij}}/\partial t)PR]$.

$B_s = \sigma_f^2 R(b_2 + b_5) - I_{1_{ij}}(PQ + [Q + (\bar{k}_{ds}R + b_5)]^2) - (\partial I_{1_{ij}}/\partial t)R(Q + (\bar{k}_{ds}R + b_5)) - (I_{4_{ij}}^{(2)} + I_{4_{ij}}^{(5)})$.

B_z Boltzmann's constant, J K^{-1}.

$\beta^* = [ik_1\bar{v} + k_ik_jD_{ij} + ((\bar{k}_c + \bar{\alpha}_c\eta_0 + \bar{k}_{ds}) + \alpha_1)] + [(\bar{k}_y + \bar{k}_{ds}) + \beta_2]$.

β_1 effective gain coefficient for free viruses, day^{-1}.

β_2 effective loss coefficient for attached viruses, day^{-1}.

C mass fraction of free viruses.

$\bar{c}$ mean free-virus concentration (mass fraction).

c' perturbation in free-virus concentration (mass fraction).

$\hat{c}$ "conservative" free-virus concentration (mass fraction).

$\chi = -(\lambda_1/\bar{v})(A_x + (B_s/B))$.

d effective grain diameter (d_{10}), m.

d_p diameter of viruses, m.

D_{ij} local dispersion tensor, m^2 d^{-1}.

D_d^* porous media molecular diffusion coefficient, m^2 d^{-1}.

dZ_c Fourier-Stieltjes amplitude for free-virus concentration.

$dZ_{\hat{c}}$ Fourier-Stieltjes amplitude for conservative free-virus concentration ($\hat{c}$).

$dZ_{\delta i}$ Fourier-Stieltjes amplitude for δ_i, $i = 1, \cdots, 5$.

dZ_f Fourier-Stieltjes amplitude for ln K.

dZ_s Fourier-Stieltjes amplitude for attached-virus concentration.

$dZ_{\hat{s}}$ Fourier-Stieltjes amplitude for conservative attached-virus concentration ($\hat{s}$).

dZ_{v_i} Fourier-Stieltjes amplitude for pore water velocity, m d^{-1}.

δ_{ij} Kronecker delta function.

δ_i random, uncorrelated portion of virus adsorption ($i = 1$), virus detachment ($i = 2$), collision efficiency ($i = 3$), free-virus inactivation ($i = 4$) and attached-virus inactivation ($i = 5$) coefficients (e.g., $k_c = a_1 + b_1 \ln K + \delta_1$).

δ_i' perturbation in δ_i ($i = 1, \cdots, 5$).

$E[\ ]$ expected value operator.

f natural logarithm of hydraulic conductivity (ln K).

$\bar{f}$ mean ln K.

f' perturbation of ln K.

$G_i = -\partial\bar{c}/\partial\zeta_i$.

g gravitational acceleration, m s^{-2}.

$\gamma = \bar{v}n/K_gJ_1$.

H Hamaker constant, J.

η single collector efficiency, day^{-1}.

$\eta^* = [3(1-n)/2d]v_i\eta$.

$\bar{\eta}^*$ mean η^*, day^{-1}.
$\eta^{*\prime}$ perturbation in η^*, day^{-1}.
$\eta_0 = K_g^{c_{10}}(a_{10} + b_{10}\bar{v}) + K_g^{c_{11}}(a_{11} + b_{11}\bar{v}) + K_g^{c_{12}}(a_{12} + b_{12}\bar{v})$.
$\eta_1 = K_g^{c_{10}}c_{10}(a_{10} + b_{10}\bar{v}) + K_g^{c_{11}}c_{11}(a_{11} + b_{11}\bar{v}) + K_g^{c_{12}}c_{12}(a_{12} + b_{12}\bar{v})$.
$\eta_2 = K_g^{c_{10}}b_{10} + K_g^{c_{11}}b_{11} + K_g^{c_{12}}b_{12}$.
$\eta_3 = \frac{1}{2}[K_g^{c_{10}}c_{10}^2(a_{10} + b_{10}\bar{v}) + K_g^{c_{11}}c_{11}^2(a_{11} + b_{11}\bar{v}) + K_g^{c_{12}}c_{12}^2(a_{12} + b_{12}\bar{v})]$.
$\eta_4 = K_g^{c_{10}}b_{10}c_{10} + K_g^{c_{11}}b_{11}c_{11} + K_g^{c_{12}}b_{12}c_{12}$.
$I_{1_{ij}} = (\sigma_f^2\lambda_1/\bar{v})(1 - \exp[-\bar{v}t/\lambda_1(\chi + 1)])/(\chi + 1)$.
$I_{4_{ij}}^{(m)} = (\sigma_{\delta m}^2\lambda_{1m}/\bar{v})(1 - \exp[-\bar{v}t/\lambda_{1m}(\chi + 1)])/(\chi + 1)$, $i = 1, \cdots, 5$.
J_1 hydraulic gradient in x_1 direction, m m^{-1}.
K hydraulic conductivity, m d^{-1}.
K_g exp ($\bar{f}$).
k_c virus adsorption coefficient, day^{-1}.
$\bar{k}_c$ mean virus adsorption coefficient, day^{-1}.
k_c' perturbation in virus adsorption coefficient, day^{-1}.
k_{dc} inactivation rate for free viruses, day^{-1}.
$\bar{k}_{dc}$ mean free-virus inactivation rate, day^{-1}.
k_{dc}' perturbation in free-virus inactivation rate, day^{-1}.
k_{ds} inactivation rate for attached viruses, day^{-1}.
$\bar{k}_{ds}$ mean attached-virus inactivation rate, day^{-1}.
k_{ds}' perturbation in attached virus inactivation rate, day^{-1}.
k_i wave number ($i = 1, 2, 3$), meter^{-1}.
k_y virus detachment rate, day^{-1}.
$\bar{k}_y$ mean virus detachment rate, day^{-1}.
k_y' perturbation in virus detachment rate, day^{-1}.
λ_i hydraulic conductivity correlation scale ($i = 1, 2, 3$), m.
λ_{i_j} δ_j correlation scale ($j = 1, \cdots, 5$) in the i direction ($i = 1, 2, 3$), m.
μ dynamic viscosity, N s m^{-2}.
n effective porosity.
n_b total porosity.
$P = b_1 + \bar{\alpha}_c\eta_1 + b_3\eta_0 + \bar{\alpha}_c\eta_2\bar{v}/\gamma$.
$Q = \bar{k}_yR + b_2$.
q_i specific discharge or Darcy flux, m d^{-1}.
$R = \rho_s a_r b_r K_g^{b_r}/\bar{r}$.
$r = \rho_b/n$.
$\bar{r}$ mean ρ_b/n.
r' perturbation in ρ_b/n.
R_{ff} covariance function of ln K field.
ρ density of solution, kg m^{-3}.
ρ_b bulk density of porous media, kg m^{-3}.
ρ_p buoyant density of viruses, kg m^{-3}.
ρ_s density of soil grains, kg m^{-3}.
S mass fraction of attached viruses.
$\bar{s}$ mean attached-virus concentration (mass fraction).
s' perturbation in attached-virus concentration (mass fraction).
$\hat{s}$ "conservative" attached-virus concentration (mass fraction).
S_{ff} spectrum of ln K field, m^3.
σ_f^2 variance of ln K field.
$\sigma_{\delta_i}^2$ variance of δ_i field ($i = 1, \cdots, 5$).
t time, d.
T temperature, K.
v_i pore water velocity, m d^{-1}.
v_e effective velocity of free viruses, m d^{-1}.
$\bar{v}$ mean pore water velocity (aligned with x_1 axis), m d^{-1}.
v_i' perturbation in pore water velocity, m d^{-1}.
x_i orthogonal distance ($i = 1, 2, 3$), m.
ξ_i separation vector, m.
ζ_i coordinate system moving with free-virus plume ($i = 1, 2, 3$), m.

Acknowledgments. This work was funded initially by a Drexel University Teaching Assistantship, Teaching Fellowship, and Society of Women Engineers' Scholarship to the first author and subsequently by National Science Foundation Hydrologic Sciences grant #EAR9725086. We are grateful to Arthur L. Baehr for his advice in implementing the finite difference code used to carry out the numerical simulations for this paper. This paper benefited greatly from the constructive review comments provided by Stanley B. Grant, three anonymous reviewers, peer reviewers for USGS, George M. Hornberger and Kathryn M. Hess, and Associate Editor Wendy D. Graham.

References

Ababou, R., D. McLaughlin, L. W. Gelhar, A. F. B. Tompson, Numerical simulation of three-dimensional saturated flow in randomly heterogeneous porous media, *Transp. Porous Media*, *4*, 549–565, 1989.

Anan'ev, N. I., and N. D. Demin, On the spread of pollutants in subsurface waters, *Hyg. Sanit.*, *36*, 292–294, 1971.

Aulenbach, D. B., Long-term recharge of trickling filter effluent into sand, *Rep. EPA-600/2-79-068*, Environ. Prot. Agency, Ada, Okla., 1979.

Bagdasar'yan, G. A., Survival of viruses of the enterovirus group (poliomyelitis, ECHO, Coxsackie) in soil and on vegetables, *J. Hyg. Epidemiol. Microbiol. Immunol.*, *7*, 497–505, 1964.

Bales, R. C., C. P. Gerba, G. H. Grondin, and S. L. Jensen, Bacteriophage transport in sandy soil and fractured tuff, *Appl. Environ. Microbiol.*, *55*, 2061–2067, 1989.

Bales, R. C., S. R. Hinkle, T. W. Kroeger, K. Stocking, and C. P. Gerba, Bacteriophage adsorption during transport through porous media: Chemical perturbations and reversibility, *Environ. Sci. Technol.*, *25*, 2088–2095, 1991.

Bales, R. C., S. Li, K. M. Maguire, M. T. Yahya, and C. P. Gerba, MS-2 and Poliovirus transport in porous media: Hydrophobic effects and chemical perturbations, *Water Resour. Res.*, *29*(4), 957–963, 1993.

Bales, R. C., S. Li, K. M. Maguire, M. T. Yahya, C. P. Gerba, and R. W. Harvey, Virus and bacteria transport in a sandy aquifer, Cape Cod, MA, *Ground Water*, *33*(4), 653–661, 1995.

Bales, R. C., S. Li, T. J. Yeh, M. E. Lenczewski, and C. P. Gerba, Bacteriophage and microsphere transport in saturated porous media: Forced-gradient experiment at Borden, Ontario, *Water Resour. Res.*, *33*(4), 639–648, 1997.

Bear, J., *Dynamics of Fluids in Porous Media*, Dover, Mineola, N. Y., 1972.

Blanc, R., and A. Nasser, Effect of effluent quality and temperature on the persistence of viruses in soil, *Water Sci. Technol.*, *33*(10–11), 237–242, 1996.

Corapcioglu, M. Y., and A. Haridas, Transport and fate of microorganisms in porous media: A theoretical investigation, *J. Hydrol.*, *72*, 149–169, 1984.

Craun, G. F., A summary of waterborne illness transmitted through contaminated groundwater, *J. Environ. Health*, *48*, 122–127, 1985.

Dagan, G., *Flow and Transport in Porous Formations*, Springer-Verlag, New York, 1989.

Davis, S. N., and R. J. M. DeWiest, *Hydrogeology*, John Wiley, New York, 1966.

Fletcher, M. W., and R. L. Myers, Groundwater tracing in karst terrain using phage T-4, paper presented at Annual Meeting, Am. Soc. of Microbiol., Chicago, Ill., 1974.

Garabedian, S. P., L. W. Gelhar, and M. A. Celia, Large-scale dispersive transport in aquifers: Field experiments and reactive transport theory, *Ralph M. Parsons Lab. Rep. 315*, Mass. Inst. of Technol., Cambridge, Mass., 1988.

Gelhar, L. W., Stochastic analysis of solute transport in saturated and unsaturated porous media, in *Advances in Transport Phenomena in Porous Media*, edited by J. Bear and M. Y. Corapcioglu, *NATO ASI Ser., Ser. E*, *128*, 657–700, 1987.

Gelhar, L. W., *Stochastic Subsurface Hydrology*, Prentice-Hall, Englewood Cliffs, N. J., 1993.

Gelhar, L. W., Perspectives on field-scale application of stochastic subsurface hydrology, in *Subsurface Flow and Transport: A Stochastic Approach*, edited by G. Dagan and S. P. Neuman, Cambridge Univ. Press, New York, 1997.

Gelhar, L. W., and C. L. Axness, Three-dimensional stochastic analysis of macrodispersion in aquifers, *Water Resour. Res.*, *19*(1), 161–180, 1983.

Gerba, C. P., C. Wallis, and J. L. Melnick, Fate of wastewater bacteria and viruses in soil, *J. Irrig. Drain. Div., Am. Soc. Civ. Eng.*, *101*(IR3), 157–174, 1975.

Gorelick, S. M., R. A. Freeze, D. Donohue, and J. F. Keely, *Groundwater Contamination: Optimal Capture and Containment*, A. F. Lewis, New York, 1993.

Harvey, R. W., Parameters involved in modeling movement of bacteria in groundwater, in *Modeling the Environmental Fate of Microorganisms*, edited by C. J. Hurst, pp. 89–114, Am. Soc. for Microbiol., Washington, D. C., 1991.

Harvey, R. W., and S. P. Garabedian, Use of colloid filtration theory in modeling movement of bacteria through a contaminated sandy aquifer, *Environ. Sci. Technol.*, *25*, 178–185, 1991.

Harvey, R. W., N. E. Kinner, D. MacDonald, D. W. Metge, and A. Bunn, Role of physical heterogeneity in the interpretation of small-scale laboratory and field observations of bacteria, microbial-sized microsphere, and bromide transport through aquifer sediments, *Water Resour. Res.*, *29*(8), 2713–2721, 1993.

Hazen, A., A discussion of "Dams on sand foundations" by A. C. Koenig, *Trans. Am. Soc. Civ. Eng.*, *73*, 199, 1911.

Hess, K. M., S. H. Wolf, and M. A. Celia, Large-scale natural gradient tracer test in sand and gravel, Cape Cod, Massachusetts, 3, Hydraulic conductivity variability and calculated macrodispersivities, *Water Resour. Res.*, *28*(8), 2011–2027, 1992.

Hornberger, G. M., A. L. Mills, and J. S. Herman, Bacterial transport in porous media: Evaluation of a model using laboratory observations, *Water Resour. Res.*, *28*(3), 915–938, 1992.

Hurst, C. J., C. P. Gerba, and I. Cech, Effects of environmental variables and soil characteristics on virus survival in soil, *Appl. Environ. Microbiol.*, *40*, 1067–1079, 1980.

Hurst, C. J., G. R. Knudsen, M. J. McInerney, L. D. Stetzenback, and M. V. Walters (eds.), *Manual of Environmental Microbiology*, Am. Soc. for Microbiol., Washington, D. C., 1997.

Idelovitch, E., et al., Dan Region Project, groundwater recharge with municipal effluent, report, Mekorot Water Co., Tel Aviv, Israel, 1979.

Jin, Y., M. V. Yates, S. S. Thompson, and W. A. Jury, Sorption of viruses during flow through saturated columns, *Environ. Sci. Technol.*, *31*, 548–555, 1997.

Johnson, P. R., N. Sun, and M. Elimelech, Colloid transport in geochemically heterogeneous porous media: Modeling and measurements, *Environ. Sci. Technol.*, *31*, 3284–3293, 1996.

Jussel, P., F. Stauffer, and T. Dracos, Three-dimensional simulation of solute transport in inhomogeneous fluvial gravel deposits using stochastic concepts, in *WR90 Computational Methods in Subsurface Hydrology, Proceedings of the 8th International Conference on Computational Methods in Water Resources*, edited by G. Gambolati et al., Springer-Verlag, New York, 1990.

Kauffman, L. J., Dispersion of dense, viscous, miscible fluids in heterogeneous porous media: Laboratory investigation and stochastic, two-dimensional mean simulations, M.S. thesis, Drexel Univ., Philadelphia, Pa., 1996.

Kinoshita, T., R. C. Bales, K. M. Maguire, and C. P. Gerba, Effect of pH on bacteriophage transport through sandy soils, *J. Contam. Hydrol.*, *14*, 55–70, 1993.

Koerner, E. L., and D. A. Haws, Long-term effects of land application of domestic wastewater: Vineland, New Jersey, rapid infiltration site, *Rep. EPA-600/2-79-072*, Environ. Prot. Agency, Washington, D. C., 1979.

Li, S. G., and D. McLaughlin, A nonstationary spectral method for solving stochastic groundwater problems: Unconditional analysis, *Water Resour. Res.*, *27*(7), 1589–1605, 1991.

Li, S. G., and D. McLaughlin, Using the nonstationary spectral method to analyze flow through heterogeneous trending media, *Water Resour. Res.*, *31*(3), 541–551, 1995.

Logan, B. E., D. G. Jewett, R. G. Arnold, E. J. Bouwer, and C. R. O'Melia, Clarification of clean-bed filtration models, *J. Environ. Eng.*, *121*(12), 869–873, 1995.

Lumley, J. L., and H. A. Panofsky, *The Structure of Atmospheric Turbulence*, Wiley-Interscience, New York, 1964.

Macler, B. A., Developing a national drinking water regulation for disinfection of groundwater, *Groundwater Monit. Rev.*, *15*(4), 77–84, 1995.

Mantoglou, A., and L. W. Gelhar, Large-scale models of transient unsaturated flow systems, *Water Resour. Res.*, *23*(1), 37–46, 1987a.

Mantoglou, A., and L. W. Gelhar, Capillary tension head, soil moisture content, and effective soil moisture capacity of transient unsaturated flow in soils, *Water Resour. Res.*, *23*(1), 47–56, 1987b.

Mantoglou, A., and L. W. Gelhar, Effective hydraulic conductivities of transient unsaturated flow in stratified soils, *Water Resour. Res.*, *23*(1), 57–67, 1987c.

Martin, G. N., and M. J. Noonan, Effects of domestic wastewater disposal by land irrigation on groundwater quality of the central Canterbury Plains, *Tech. Publ. 7*, Water and Soil Div., Minist. of Works and Dev., Christchurch, New Zealand, 1977.

Martin, M. J., B. E. Logan, W. P. Johnson, D. G. Jewett, and R. G. Arnold, Scaling bacterial filtration rates in different sized porous media, *J. Environ. Eng.*, *122*(5), 407–415, 1996.

Martin, R., and A. Thomas, An example of the use of bacteriophage as a groundwater tracer, *J. Hydrol.*, *23*, 73–78, 1974.

Martin, R. E., E. J. Bouwer, and L. M. Hanna, Application of clean-bed filtration theory to bacterial deposition in porous media, *Environ. Sci. Technol.*, *26*, 1053–1058, 1992.

Matthess, G., A. Pekdeger, and J. Schroeter, Persistence and transport of bacteria and viruses in groundwater—A conceptual evaluation, *J. Contam. Hydrol.*, *2*, 171–188, 1988.

McKay, L. D., J. A. Cherry, R. C. Bales, M. T. Yahya, and C. Gerba, A field example of bacteriophage as tracers of fracture flow, *Environ. Sci. Technol.*, *27*, 1075–1079, 1993a.

McKay, L. D., R. W. Gilham, and J. A. Cherry, Field experiments in fractured clay till, 2, Solute and colloid transport, *Water Resour. Res.*, *29*(12), 3879–3890, 1993b.

Miralles-Wilhelm, F., and L. W. Gelhar, Stochastic analysis of sorption macrokinetics in heterogeneous aquifers, *Water Resour. Res.*, *32*(6), 1541–1549, 1996a.

Miralles-Wilhelm, F., and L. W. Gelhar, Stochastic analysis of transport and decay of a solute in heterogeneous aquifers, *Water Resour. Res.*, *32*(12), 3451–3459, 1996b.

Morley, L. M., G. M. Hornberger, A. L. Mills, and J. S. Herman, Effects of transverse mixing on transport of bacteria through heterogeneous porous media, *Water Resour. Res.*, *34*(8), 1901–1908, 1998.

Naff, R. L., A continuum approach to the study and determination of field longitudinal dispersion coefficients, Ph.D. dissertation, N. M. Inst. of Min. and Technol., Socorro, 1978.

Neuman, S. P., Stochastic approach to subsurface flow and transport: A view to the future, in *Subsurface Flow and Transport: A Stochastic Approach*, edited by G. Dagan and S. P. Neuman, pp. 231–241, Cambridge Univ. Press, New York, 1997.

New Jersey Department of Environmental Protection, Water for the 21st century: The vital resource. N. J. Statewide Water Supply Plan, Off. of Environ. Plann., August, 1996.

Noonan, M. J., and J. F. McNabb, Contamination of Canterbury groundwater by viruses, in *The Quality and Movement of Groundwater in Alluvial Aquifers of New Zealand*, *Tech. Publ. 2*, edited by M. M. Noonan, pp. 195–210, Dep. of Agric. Microbiol., Lincoln Coll., Canterbury, New Zealand, 1979.

Park, N.-S., T. N. Blanford, and P. S. Huyakorn, VIRALT: A model for simulating viral transport in groundwater, documentation and user's guide, version 2.0, Hydrogeol., Inc., Herndon, Va., 1991.

Penrod, S. L., T. M. Olson, and S. B. Grant, The deposition kinetics of two viruses in packed beds of quartz granular media, *Langmuir*, *12*, 5576–5587, 1996.

Pieper, A. P., J. N. Ryan, R. W. Harvey, G. L. Amy, T. H. Illangasekare, and D. W. Metge, Transport and recovery of bacteriophage

PRD1 in an unconfined sand aquifer: Effect of sewage-derived organic matter, *Environ. Sci. Technol.*, *31*, 1163–1170, 1997.

Powelson, D. K., C. P. Gerba, and M. T. Yahya, Virus transport and removal in wastewater during aquifer recharge, *Water Res.*, *27*(4), 583–590, 1993.

Rajagopalan, R., and C. Tien, Trajectory analysis of deep-bed filtration with the sphere-in-cell porous media model, *AIChE J.*, *22*(3), 523–533, 1976.

Redman, J. A., S. B. Grant, T. M. Olson, M. E. Hardy, and M. K. Estes, Filtration of recombinant Norwalk virus particles and bacteriophage MS2 in quartz sand: Importance of electrostatic interactions, *Environ. Sci. Technol.*, *31*, 3378–3383, 1997.

Rehmann, L. L. C., A spectral stochastic model of virus transport in aquifers, Ph.D. thesis, 225 pp., Drexel Univ., Philadelphia, Pa., 1998.

Saiers, J. E., G. M. Hornberger, and L. Liang, First- and second-order kinetics approaches for modeling the transport of colloidal particles in porous media, *Water Resour. Res.*, *30*(9), 2499–2506, 1994.

Schaub, S. A., and C. A. Sorber, Virus and bacteria removal from wastewater by rapid infiltration through soil, *Appl. Environ. Microbiol.*, *33*, 609–619, 1977.

Schijven, J. F., W. Hoogenboezem, J. H. Peters, and S. M. Hassanizadeh, Removal of bacteriophage by dune infiltration: Field studies and modeling, *Eos Trans. AGU*, *78*(46), Fall Meet. Suppl., F212, 1997.

Scholl, M. A., and R. W. Harvey, Laboratory investigations on the role of sediment surface and groundwater chemistry in transport of bacteria through a contaminated sandy aquifer, *Environ. Sci. Technol.*, *26*, 1410–1417, 1992.

Sim, Y., and C. V. Chrysikopoulos, One-dimensional virus transport in porous media with time-dependent inactivation rate coefficients, *Water Resour. Res.*, *32*(8), 2607–2611, 1996.

Skilton, H., and D. Wheeler, Bacteriophage tracer experiments in groundwater, *J. Appl. Bacteriol.*, *65*, 387–395, 1988.

Sobsey, M. D., C. H. Dean, M. E. Knuckles, and R. A. Wagner, Interactions and survival of enteric viruses in soil materials, *Appl. Environ. Microbiol.*, *40*, 92–101, 1980.

Sobsey, M. D., P. A. Shields, F. H. Hauchman, R. L. Hazard, and L. W. Caton III, Survival and transport of hepatitis A virus in soils, groundwater and wastewater, *Water Sci. Technol.*, *18*(10), 97–106, 1986.

Tim, U. S., and S. Mostaghimi, Model for predicting virus movement through soils, *Ground Water*, *29*(2), 251–259, 1991.

Tompson, A. F. B., and L. W. Gelhar, Numerical simulation of solute transport in randomly heterogeneous porous media, *Water Resour. Res.*, *26*(10), 2541–2562, 1990.

Toran, L., and A. V. Palumbo, Colloid transport through fractured and unfractured laboratory sand columns, *J. Contam. Hydrol.*, *9*, 289–303, 1992.

U.S. Army Corps of Engineers, Evaluation of procedures for determining selected aquifer parameters, *Rep. 82-41*, Cold Reg. Res. and Eng. Lab., Hanover, N. H., 1982.

U.S. Environmental Protection Agency, Draft groundwater disinfection rule, *Rep. 811/P-92-001*, Off. of Ground Water and Drink. Water, Washington, D. C., 1992.

Vaughn, J., and E. F. Landry, Data report: An assessment of the occurrence of human viruses in Long Island aquatic systems, *Rep. BNL 50787*, Brookhaven Natl. Lab., Dep. of Energy and Environ., Upton, N. Y., 1977.

Welty, C., and L. W. Gelhar, Stochastic analysis of the effects of fluid density and viscosity variability on macrodispersion in heterogeneous porous media, *Water Resour. Res.*, *27*(8), 2061–2076, 1991.

Wollum, A. G., and D. K. Cassel, Transport of microorganisms in sand columns, *Soil Sci. Soc. Am. J.*, *42*, 72–76, 1978.

Yao, K. M., M. T. Habibian, and C. R. O'Melia, Water and waste water filtration: Concepts and applications, *Environ. Sci. Technol.*, *5*(11), 1105–1112, 1971.

Yates, M. V., Field evaluation of the GWDR's natural disinfection criteria, *J. Am. Water Works Assoc.*, *86*(2), 76–85, 1995.

Yates, M. V., and S. R. Yates, Modeling microbial transport in soil and groundwater, *ASM News*, *56*(6), 324–327, 1990.

Yates, M. V., C. P. Gerba, and L. M. Kelley, Virus persistence in groundwater, *Appl. Environ. Microbiol.*, *49*, 778–781, 1985.

L. L. Campbell Rehmann, 875 Central Avenue, Hammonton, NJ 08037. (llcr@erols.com)

R. W. Harvey, Water Resources Division, U.S. Geological Survey, 3215 Marine Street, Room E119, Boulder, CO 80303. (rwharvey@usgs.gov)

C. Welty, School of Environmental Science, Engineering, and Policy, Drexel University, Philadelphia, PA 19104. (weltyc@post.drexel.edu)

(Received June 24, 1998; revised February 17, 1999;
accepted March 1, 1999.)